Structure−Affinity Relationships (SARs) and Structure−Kinetics Relationships (SKRs) of K$_v$11.1 Blockers

Zhiyi Yu,[†] Jacobus P. D. van Veldhoven,[†] Julien Louvel,[†] Ingrid M. E. 't Hart,[†] Martin B. Rook,[‡] Marcel A. G. van der Heyden,[‡] Laura H. Heitman,[†] and Adriaan P. IJzerman*,[†]

[†]Division of Medicinal Chemistry, Leiden Academic Centre for Drug Research, Leiden University, 2300 RA Leiden, The Netherlands

[‡]Department of Medical Physiology, Division Heart & Lungs, University Medical Centre Utrecht, 3584 CM Utrecht, The Netherlands

Ⓢ *Supporting Information*

ABSTRACT: K$_v$11.1 (hERG) blockers with comparable potencies but different binding kinetics might display divergent pro-arrhythmic risks. In the present study, we explored structure−kinetics relationships in four series of K$_v$11.1 blockers next to their structure−affinity relationships. We learned that despite dramatic differences in affinities and association rates, there were hardly any variations in the dissociation rate constants of these molecules with residence times (RTs) of a few minutes only. Hence, we synthesized 16 novel molecules, in particular in the pyridinium class of compounds, to further address this peculiar phenomenon.

compound 37
K$_i$ = 498 ± 107 nM
k$_{on}$ = 0.0086 ± 0.0020 nM^{-1}·min^{-1}
Residence time = 0.34 ± 0.04 min

compound 38
K$_i$ = 86 ± 12 nM
k$_{on}$ = (7.5 ± 1.0)×10^{-5} nM^{-1}·min^{-1}
Residence time = 105 ± 4 min

Differential kinetics of K$_v$11.1 (hERG) blockers

We found molecules with very short RTs (e.g., 0.34 min for **37**) and much longer RTs (e.g., 105 min for **38**). This enabled us to construct a $k_{on}−k_{off}−K_D$ kinetic map for all compounds and subsequently divide the map into four provisional quadrants, providing a possible framework for a further and more precise categorization of K$_v$11.1 blockers. Additionally, two representative compounds (**21** and **38**) were tested in patch clamp assays, and their RTs were linked to their functional IC$_{50}$ values. Our findings strongly suggest the importance of the simultaneous study of ligand affinities and kinetic parameters, which may help to explain and predict K$_v$11.1-mediated cardiotoxicity.
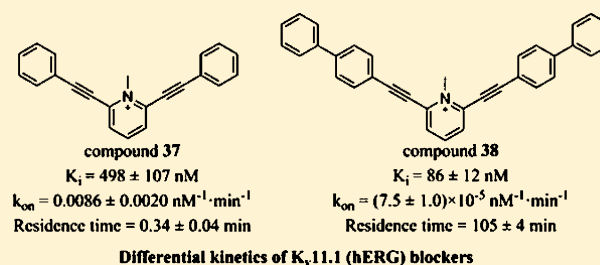
INTRODUCTION

Cardiac safety has become a major concern facing the pharmaceutical industries and regulatory agencies over the last several decades. A substantial number of drugs, including both cardiac and noncardiac medications, have been restricted in their applications or withdrawn from the market due to their K$_v$11.1-induced cardiotoxicity.[1,2] The K$_v$11.1 channel, often referred to as the human ether-à-go-go-related gene (hERG) K$^+$ channel, mediates the most important component of phase 3 repolarization of human ventricular myocytes.[3] Blockade of the K$_v$11.1 channel can lead to the prolongation of action potential durations (APDs) and an elevated risk of lethal arrhythmias such as Torsade de Pointes (TdP).[4] As a consequence, measurement of K$_v$11.1 liabilities of drugs is a critical component of regulatory guidelines for preclinical QT studies.[5,6] In this regard, a 30-fold safety margin between K$_v$11.1 IC$_{50}$ and C_{max} values (maximum free plasma concentrations) has been proposed to define the cardiac safety of compounds.[7] However, this approach of considering IC$_{50}$ values solely is rather arbitrary and crude, which might explain unsatisfactory quantitative predictions and sometimes excludes useful medications that are not problematic.[6,8,9] For instance, the IC$_{50}$ value of ketoconazole (1-[4-(4-{[(2R,4S)-2-(2,4-dichlorophenyl)-2-(1H-imidazol-1-ylmethyl)-1,3-dioxolan-4-yl]methoxy}phenyl)piperazin-1-yl]ethan-1-one) at the K$_v$11.1 channel is relatively close to its effective therapeutic plasma concentration (11-fold difference), yet it has been proven to be a safe drug in clinical trials due to the fact that this drug has a slow binding rate and is not trapped into the channel.[9,10] Therefore, knowledge of association and dissociation kinetics of drugs at the K$_v$11.1 channel may be important in defining their propensities to prolong the QT interval.

The concept of structure−affinity relationships (SARs) describing the interdependency between compound structures and binding affinities has been extensively explored over the past decades.[11,12] However, similar studies illustrating the dependency between compound structures and binding kinetics, coined as structure−kinetics relationships (SKRs) have been less well investigated to date. Recently, drug−target kinetics, in particular receptor−ligand residence times (RTs), have been shown to also determine the therapeutic potential of drug candidates in vivo and to be predictive of drug efficacy and safety.[13,14] Consequently, there is an emerging awareness of the importance of measuring the kinetics of drug−target interactions. SKRs are now being reported and discussed for ligand binding to G protein-coupled receptors (GPCRs) and enzymes.[11,15−17] With regard to ion channels, measuring the interaction kinetics of drugs with the K$_v$11.1 channel has already been recommended to be incorporated into compre-

Scheme 1. Synthesis of Clofilium Derivatives (19 and 20)[a]
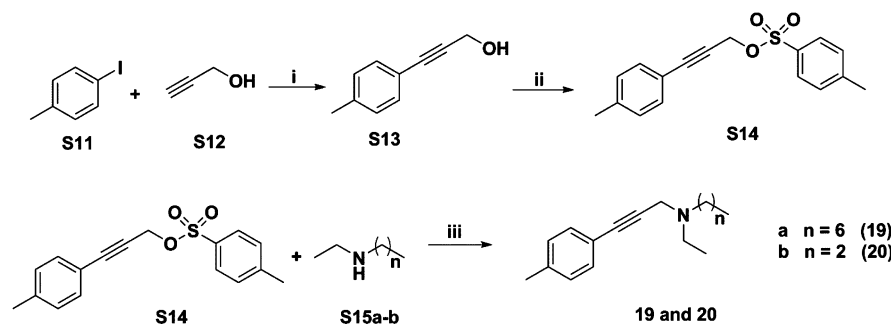
[a](i) PdCl$_2$(PPh$_3$)$_2$, CuI, Et$_3$N, THF, rt; (ii) tosyl chloride, KOH, Et$_2$O, 0 °C to rt; (iii) K$_2$CO$_3$, DMF, rt.

Scheme 2. Synthesis of Symmetrical 2,6-Substituted *N*-Methylated Pyridines with Various Alkyl Chain Lengths[a]
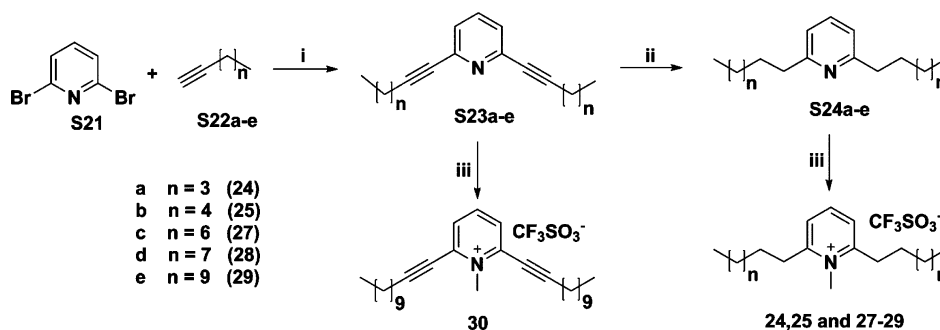
[a](i) PdCl$_2$(PPh$_3$)$_2$, CuI, Et$_3$N, rt; (ii) 10% Pd/C, H$_2$, THF, MeOH, rt; (iii) CF$_3$SO$_2$OCH$_3$, CH$_2$Cl$_2$, 0 °C to rt.

hensive in vitro proarrhythmia assay (CiPA) strategies to hopefully provide significant improvements of proarrhythmic assessments.[18,19] Recent studies have demonstrated that K$_v$11.1 blockers with similar potencies (IC$_{50}$ values) but distinct binding kinetics can have markedly diverse proarrhythmic potential, suggesting the necessity to extend K$_v$11.1 inhibition assays with studies on investigating the dynamics of drug–channel interactions.[1,8,9] In addition, particular interest has arisen in the so-called trapping phenomenon, characterized by capture of a drug within the K$_v$11.1 channel and thus a slow dissociation rate from the channel, which harbors an enhanced proarrhythmic risk caused by the drug.[20,21] Moreover, a substantial underestimation of cardiac risks has been observed in assessing the ventricular action potential due to neglecting drug-binding kinetics at cardiac K$_v$11.1 channels.[8] Therefore, there is an urgent need to add the dimension of binding and unbinding kinetics to the more routinely determined affinity values in order to evaluate the arrhythmogenic potential of drug candidates in vitro.

In our previous studies, we have successfully validated a [³H]dofetilide competition association assay that can determine the association/dissociation rates and RTs of compounds accurately and efficiently.[2] In the present study, a structurally diverse set of K$_v$11.1 blockers with four different scaffolds were newly synthesized or selected from our in-house library published previously,[22−25] and their kinetic parameters (k_{on}, k_{off} K_D and RTs) as well as affinities (K_i) were determined in [³H]dofetilide binding assays. A k_{on}−k_{off}−K_D "kinetic map" was delineated for all compounds, together with three reference compounds: astemizole (1-[(4-fluorophenyl)methyl]-*N*-[1-[2-(4-methoxyphenyl)ethyl]-4-piperidyl]benzoimidazol-2-amine, a notorious K$_v$11.1 blocker withdrawn from the market), dofetilide (*N*-[4-(2-{[2-(4-methane sulfonamidophenoxy)-

ethyl](methyl)amino}ethyl)phenyl]methanesulfonamide, a specific K$_v$11.1 blocker with restricted use), and ranolazine ((*RS*)-*N*-(2,6-dim-ethylphenyl)-2-[4-[2-hydroxy-3-(2-methoxy-phenoxy)-propyl]pipe-razin-1-yl]acetamide, a safe K$_v$11.1 blocker).[2,26−28] Two compounds were further tested in a manual patch clamp assay. The SARs and SKRs derived for the compounds in this study reveal new features and aspects of the blockers' interactions with the K$_v$11.1 channel. This information is expected to provide valuable information for circumventing K$_v$11.1-induced cardiotoxicity during the preclinical stages of the drug discovery pipeline.

■ RESULTS AND DISCUSSION

Chemistry. Compounds **19**, **20**, **24**, **25**, **27−30**, and **39−46** were newly synthesized in order to obtain compounds with various RT values besides a diverse range of K_i and k_{on} values. All other compounds were selected from our in-house library based on their distinct affinities and kinetic parameters, and synthesis of these compounds has been reported in our previously published studies.[22−25]

As shown in Scheme 1, clofilium (4-(4-chlorophenyl)butyl-diethyl-heptylammonium) derivatives **19** and **20** were prepared from 4-iodotoluene in a three-step sequence as follows: Sonogashira cross-coupling of 4-iodotoluene and propargyl alcohol, formation of the corresponding tosylate, and displacement of the tosylate with the corresponding secondary amine.[24]

To investigate the effect of flexibility in the side chains of aliphatic pyridinium derivatives, several symmetrical 2,6-substituted *N*-methylated-pyridine compounds with different alkyl chain lengths (**24**, **25**, and **27−30**) were synthesized according to Scheme 2. The first series of compounds (**S23a−e**) were derived from commercially available 2,6-dibromo-pyridine and 1-alkynes with various lengths via a Sonogashira

Scheme 3. Synthesis of Symmetrical 2,6-Substituted *N*-Methylated Pyridines with Different Biphenyl Substituents[a]
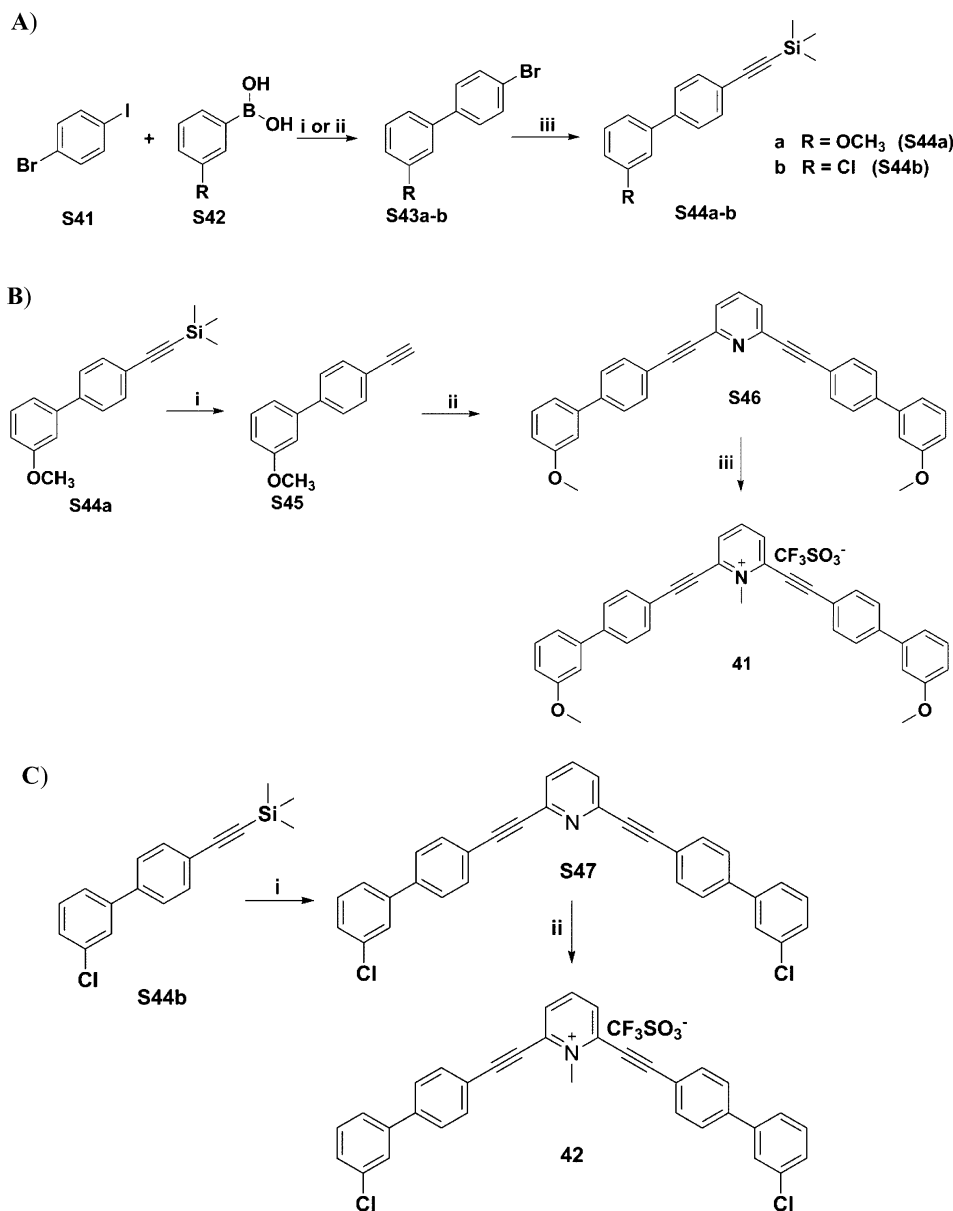

a R = 2-CH₃ (39)
b R = 3-CH₃ (40)
c R = 4-CH₃ (43)
d R = 4-OCH₃ (44)
e R = 4-Cl (46)
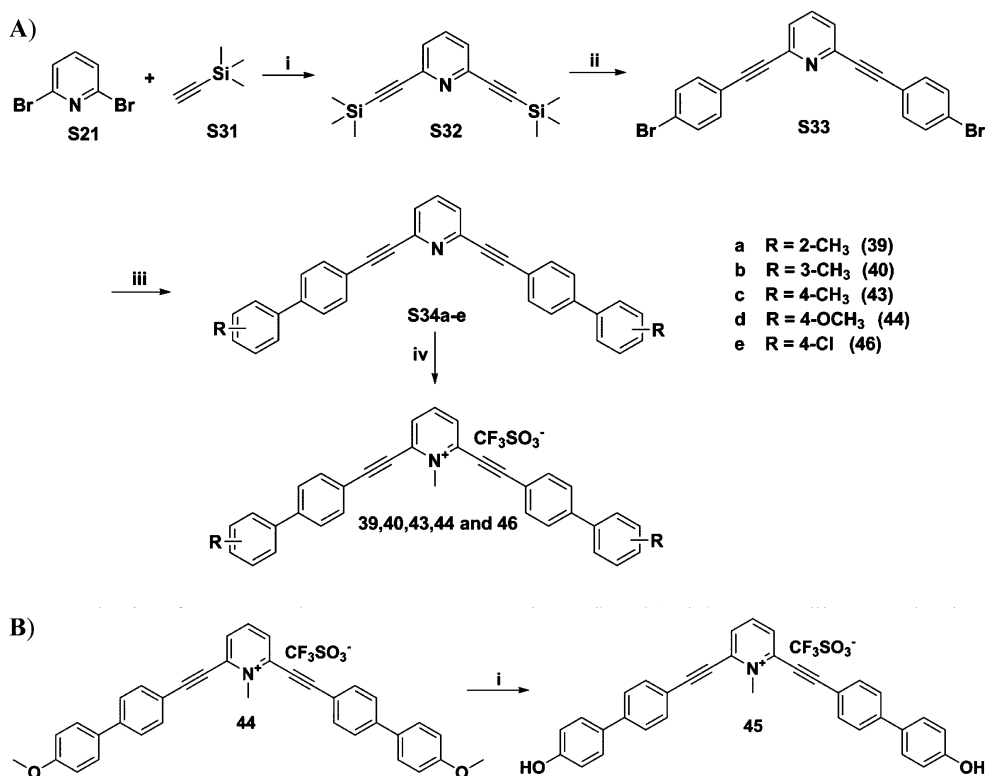
[a](A) Synthesis of compounds **39**, **40**, **43**, **44**, and **46**: (i) Pd(PPh₃)₄, CuI, diisopropylamine, toluene, rt; (ii) CuCl, PPh₃, potassium benzoate, 1-bromo-4-iodobenzene, DMI, 120 °C; (iii) Pd(PPh₃)₄, K₂CO₃, toluene, ethanol, substituted-phenylboronic acid, 50 °C; (iv) CF₃SO₂OCH₃, CH₂Cl₂, 0 °C to rt. (B) Synthesis of compound **45**: (i) BBr₃, CH₂Cl₂, −78 °C to rt.

coupling reaction.[25] The final compounds (**24**, **25**, and **27−29**) were synthesized in relatively high yields by reduction of triple bonds to single bonds and methylation of neutral pyridines. **30** was obtained directly from **S23e** by methylation of the central nitrogen with a good yield of 94%.

Next, influences of different substituents at the phenyl rings on affinities and kinetic parameters of $K_v11.1$ blockers were explored, and a series of substituted biphenylpyridines (**39−46**) were synthesized. As displayed in Scheme 3, compound **S32** was obtained by Sonogashira reaction of 2,6-dibromo-pyridine and ethynyltrimethylsilane with Pd(PPh₃)₄ and CuI as catalysts instead of PdCl₂(PPh₃)₂ and CuI displayed in Scheme 2.[29] After one-pot deprotection and Castro−Stephens coupling with 1-bromo-4-iodobenzene,[30] **S32** was converted to **S33** in a low yield that was probably caused by formation of undesired oxidative Glaser homocoupling and intrapolymerization of reacting molecules.[31] Suzuki reactions were further performed with **S33** and different substituted phenylboronic acids to yield the neutral pyridine compounds (**S34a−e**),[32] from which final compounds (**39**, **40**, **43**, **44**, and **46**) were derived via methylation of the central nitrogen in moderate to high yields. Subsequently, demethylation of **44** with boron tribromide led to the formation of compound **45**. Notably, synthetic routes mentioned above were not suitable for producing neutral biphenylpyridines with methoxy and chlorine substituents at the meta-position of the second benzene ring. Hence, **41** and **42** were synthesized by different methods shown in Scheme 4. In the first step, Suzuki reactions were applied between the substituted phenylboronic acid and 1-bromo-4-iodobenzene in the presence of different palladium catalysts to produce **S43a**

and **S43b** in moderate yields of 27% and 40%, respectively. **S43a** and **S43b** further reacted with ethynyltrimethylsilane through Sonogashira reaction,[33] resulting in high yields of **S44a** and **S44b**. Compound **41** was eventually obtained from **S44a** with a yield of 36% through three steps: deprotection, Sonogashira reaction, and methylation, whereas **42** was obtained from **S44b** via a one-pot Sonogashira reaction and methylation in a yield of 45%.

Biology. The binding affinities and kinetic parameters of all compounds were determined in [³H]dofetilide competitive displacement and competition association assays on HEK293 cell membranes stably transfected with the $K_v11.1$ channel (HEK293 $K_v11.1$) as described previously by our group.[2] As shown in Figure 1, compounds with a wide range of IC₅₀ values demonstrated a monophasic binding behavior instead of a biphasic pattern reported for a [³H]astemizole binding assay,[23,25] indicating that the binding process of compounds followed a single-step bimolecular interaction scheme and thus fulfilled the theoretical requirements for the Motulsky−Mahan approach to evaluate the binding kinetics of unlabeled ligands.[34] Figure 2 shows the competition association assay for three representative compounds (**31**, **37**, and **38**) with different binding kinetics, in particular varying RTs. Compound **37** had a shorter RT than [³H]dofetilide with an association curve slowly and monotonically approaching equilibrium versus time, whereas **38** possessed a longer RT compared to the radioligand, indicated by a typical "overshoot" and then a decline in the association curve.[15] Meanwhile, **31** exhibited a RT similar to dofetilide, evidenced by the same curve shape compared to the association curve of radioligand alone. As the K_i values of all

Scheme 4. Synthesis of Symmetrical 2,6-Substituted *N*-Methylated Pyridines (41 and 42)[a]

[a](A) Synthesis of compounds **S44a–b**: (i) 2 M K_2CO_3, Pd(PPh$_3$)$_4$, toluene, ethanol, 80 °C; (ii) 2 M K_2CO_3, Pd(OAc)$_2$, PPh$_3$, toluene, ethanol, 80 °C; (iii) PdCl$_2$(PPh$_3$)$_2$, CuI, PPh$_3$, THF, piperidine, 120 °C. (B) Synthesis of compound **41**: (i) 2 M NaOH, diethyl ether, methanol; (ii) PdCl$_2$(PPh$_3$)$_2$, CuI, Et$_3$N, 2,6-dibromo-pyridine; (iii) CF$_3$SO$_2$OCH$_3$, CH$_2$Cl$_2$, 0 °C to rt. (C) Synthesis of compound **42**: (i) CuCl, PPh$_3$, potassium benzoate, 2,6-dibromo-pyridine, DMI, 120 °C; (ii) CF$_3$SO$_2$OCH$_3$, CH$_2$Cl$_2$, 0 °C to rt.

tested compounds calculated from the IC$_{50}$ values mentioned above[35] were in good agreement with kinetically derived K_D data ($K_D = k_{off}/k_{on}$, Figure 3A), only K_i values were used to summarize the SARs in this study. The consistency of K_i and K_D values extended our previous finding to a more general observation,[2] proving the reliability of the [³H]dofetilide competition association assay in assessing the kinetics of unlabeled ligands at the K$_v$11.1 channel. In addition, the k_{on} values for all ligands were significantly correlated to their K_i values ($P < 0.0001$, Figure 3B), which is in agreement with our published data.[2] In the same publication affinities and kinetic parameters of parent compounds in the present study, dofetilide, E-4031, and clofilium, were also measured and reported.[2] Furthermore, a provisional k_{on}–k_{off}–K_D "kinetic map" was constructed based on the compounds' varying

affinities and kinetic parameters in order to divide these compounds into four different groups (quadrants) of potentially negligible (quadrant **IV**), moderate (quadrant **I** and **III**), and high arrhythmic (quadrant **II**) side effects (Figure 4). Finally, we selected two compounds (**21** and **38**) with comparable binding affinities but distinct association and dissociation rates or RTs to be studied in a whole-cell patch clamp assay using the same HEK293 K$_v$11.1 cells (Figure 5).

Structure–Affinity Relationships (SARs) and Structure–Kinetics Relationships (SKRs). *Derivatives of Dofetilide.* First, we explored the effects of pK_a values of the central nitrogen on affinities, association rates, and RTs of compounds **1–8** (Table 1), in which the pK_a values were taken from our previous publication.[22] Briefly, increasing the pK_a values via different *N*-alkyl substituents resulted in an increase of affinities
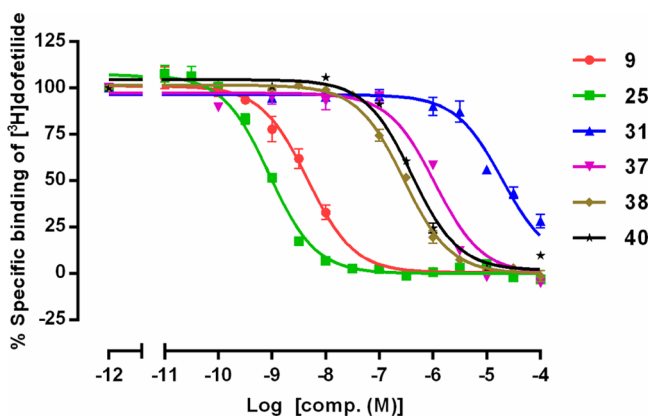
Figure 1. Representative displacement curves of specific [³H]dofetilide binding by **9**, **25**, **31**, **37**, **38**, and **40**. Experiments were performed at 25 °C using 20 μg of HEK293 K_v11.1 membrane protein. Data shown are from at least three independent experiments performed in duplicate.

Figure 2. Representative competition association curves of [³H]-dofetilide in the absence (control) or presence of unlabeled **31**, **37**, and **38** at their IC_{50} value concentrations. Experiments were performed at 25 °C using 20 μg of HEK293 K_v11.1 membrane protein. Data shown are from at least three independent experiments performed in duplicate.
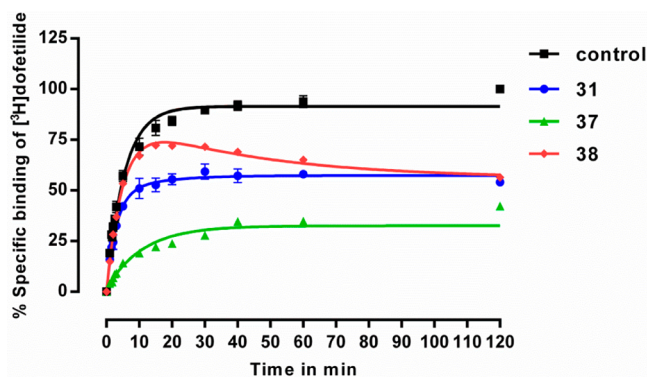
of these compounds (**1**−**5**, **7**, and **8**) at the K_v11.1 channel. Association rates of these compounds were less sensitive to pK_a alterations but showed a similar trend as the affinities. For instance, compound **8** (pK_a = −4.95) displayed the lowest affinity and smallest k_{on} value, while **3** (pK_a = 9.61) had the highest affinity and fastest association rate at the channel. These changes corresponded rather well with the principle that reducing pK_a values of the central nitrogen of K_v11.1 blockers decreases the proportion of molecules in the protonated form at physiological pH and further make fewer active species available for the productive π−cation interactions with amino acid Tyr652 lining the inner cavity of the channel.[36,37] Additionally, zwitterionic compound **6** with a CH_2COOH substituent at the central nitrogen had a lower affinity and slower association rate than **8**, indicating that the negatively charged carboxylate group caused unfavorable interactions of the K_v11.1 blocker with the channel.[38] Overall, however, the RTs ($1/k_{off}$) of **1**−**8** were not much impacted by pK_a values of the central nitrogen and zwitterionic propensity of molecules, with values between 0.56 ± 0.06 (**7**) and 3.8 ± 1.0 min (**3**).

Next, the lengths of side alkyl linkers and substituents on the phenyl rings were investigated for the analysis of SARs and SKRs. Comparable to our own studies on distance-related
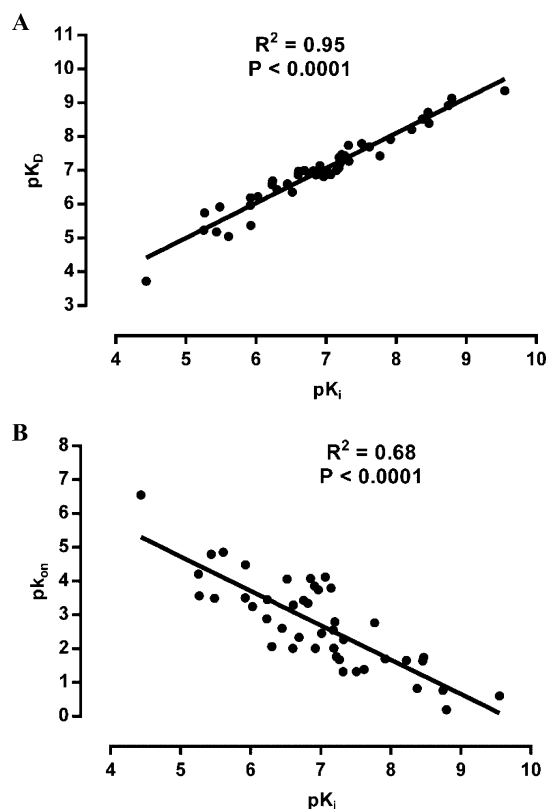

Figure 3. Correlation between pK_i and pK_D (A) or pk_{on} (B) values of all tested compounds as obtained from [³H]dofetilide competitive displacement experiments and competition association assays, respectively.
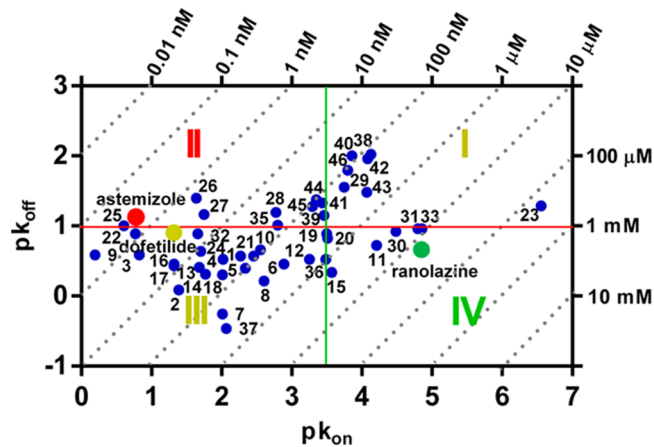

Figure 4. Kinetic map of all tested compounds in which the dissociation rate (pk_{off}, k_{off}: min^{-1}) is plotted on the y axis, whereas the association rate (pk_{on}, k_{on}: $nM^{-1}\cdot min^{-1}$) is plotted on the x axis. Identical K_D values can result from different combinations of k_{on} and k_{off} values ($K_D = k_{off}/k_{on}$, diagonal dashed lines). Quadrants (**I**, **II**, **III**, **IV**) are arbitrarily defined by red horizontal and green vertical lines according to the varied k_{on}, k_{off} and K_D values in combination with three reference compounds astemizole (red dot), dofetilide (yellow dot), and ranolazine (green dot). The intersection of red and green lines are arranged on the diagonal dashed line representing a K_D value of 316 nM, while their intercepts with y and x axis are 1 (RT = 10 min) and 3.5 (k_{on} = 3.2 × 10^{-4} $nM^{-1}\cdot min^{-1}$), respectively. Note that the kinetic parameters of compound **34** could not be determined due to its rather low K_v11.1 affinity and thus is excluded in this map.
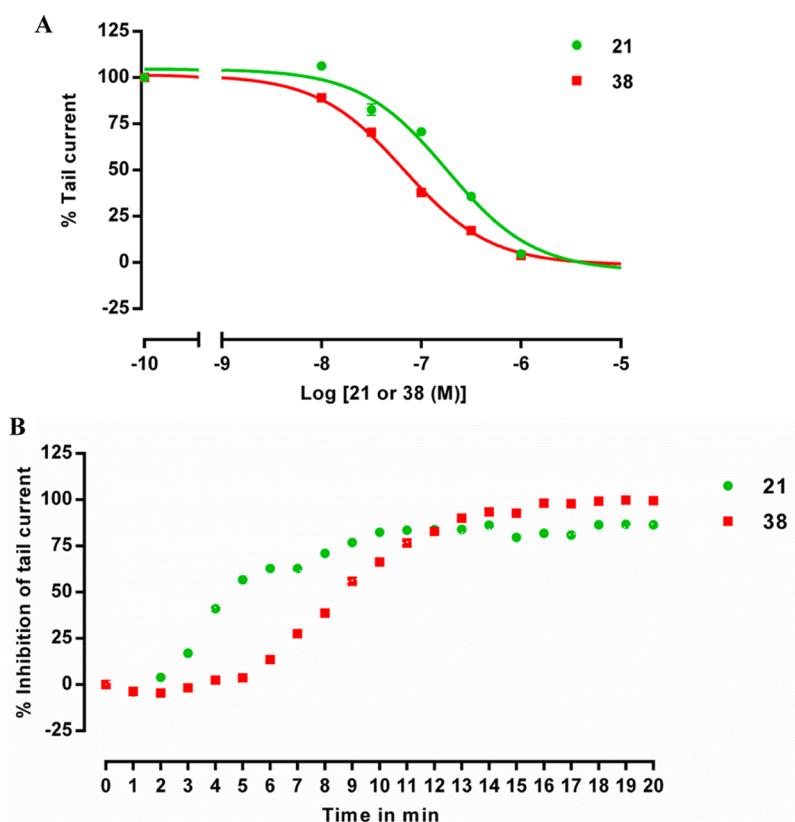
Figure 5. (A) Concentration-dependent inhibition of **21** and **38** for the $K_v11.1$ tail current in electrophysiological experiments. (B) Time-dependent inhibition of the $K_v11.1$ tail current by **21** and **38** (1 μM). Experiments were performed at room temperature using HEK293 $K_v11.1$ cells. Data shown are from at least three independent experiments.

**Table 1. Binding Affinities and Kinetic Parameters of Dofetilide Derivatives**

compd	R_1	R_2	R_3	n_1	n_2	K_i (nM)	k_{on} (nM^{-1}·min^{-1})	k_{off} (min^{-1})	K_D (nM)	RT (min)
1	4-NO$_2$	4-NO$_2$	H	2	2	47 ± 1	0.0054 ± 0.0015	0.27 ± 0.06	53 ± 6	3.7 ± 0.8
2	4-NO$_2$	4-NO$_2$	CH$_3$	2	2	24 ± 2	0.041 ± 0.004	0.82 ± 0.09	20 ± 4	1.2 ± 0.1
3	4-NO$_2$	4-NO$_2$	CH$_2$CH$_3$	2	2	4.2 ± 0.5	0.15 ± 0.06	0.26 ± 0.07	3.0 ± 0.2	3.8 ± 1.0
4	4-NO$_2$	4-NO$_2$	CH$_2$CH$_2$F	2	2	65 ± 13	0.0096 ± 0.0019	0.30 ± 0.08	41 ± 11	3.3 ± 0.9
5	4-NO$_2$	4-NO$_2$	CH$_2$CN	2	2	203 ± 6	0.0046 ± 0.0012	0.40 ± 0.05	99 ± 26	2.5 ± 0.3
6	4-NO$_2$	4-NO$_2$	CH$_2$COOH	2	2	588 ± 31	0.0013 ± 0.0001	0.35 ± 0.10	260 ± 52	2.9 ± 0.8
7	4-NO$_2$	4-NO$_2$	COCH$_3$	2	2	251 ± 32	0.0098 ± 0.0034	1.8 ± 0.2	132 ± 5	0.56 ± 0.06
8	4-NO$_2$	4-NO$_2$	COCF$_3$	2	2	355 ± 14	0.0025 ± 0.0003	0.61 ± 0.09	247 ± 27	1.6 ± 0.3
9	4-NO$_2$	4-NO$_2$	CH$_3$	4	2	1.6 ± 0.3	0.64 ± 0.29	0.26 ± 0.05	0.73 ± 0.39	3.8 ± 0.7
10	4-NO$_2$	4-NO$_2$	CH$_3$	4	1	66 ± 6	0.0028 ± 0.0008	0.22 ± 0.05	85 ± 7	4.5 ± 1.0
11	3,4-di-Cl	3,4-di-Cl	CH$_3$	2	2	5571 ± 507	(6.2 ± 3.0)x10^{-5}	0.19 ± 0.01	5807 ± 228	5.3 ± 0.2
12	H	4-OCH$_3$	CH$_3$	2	2	944 ± 58	(5.6 ± 0.9)x10^{-4}	0.30 ± 0.07	591 ± 197	3.3 ± 0.7

flexibility,[24,39] elongation of the alkyl chain between the central nitrogen and phenoxy moiety enhanced the $K_v11.1$ affinities and association rates (**9** versus **2**) while shortening the other alkyl linker with the phenyl ring lowered the affinities and association rates (**10** versus **2** and **9**). Nonetheless, **9** (RT = 3.8 ± 0.7 min) and **10** (RT = 4.5 ± 1.0 min) demonstrated similar dissociation characteristics at the $K_v11.1$ channel compared to other compounds in Table 1, suggesting that varying chain lengths between the central nitrogen and the two peripheral aromatic rings exerted negligible effects on the dissociation process of this type of ligands from the $K_v11.1$ channel. In addition, replacement of NO$_2$ groups on the phenoxy and phenyl rings with 3,4-di-Cl or other groups like OCH$_3$ dramatically decreased the $K_v11.1$ affinities and association rates of ligands (**11** and **12** versus **2**). Compound **11** had the lowest affinity (K_i = 5571 ± 507 nM), slowest association rate (k_{on} = 6.2 ± 3.0) × 10^{-5} nM^{-1}·min^{-1}), but longest RT of 5.3 ± 0.2 min at the $K_v11.1$ channel among all dofetilide derivatives (**1**−**12**). This implies that addition of electron-withdrawing groups on the aromatic rings reduces the affinities and association kinetics of $K_v11.1$ blockers by hampering their π-stacking and hydrophobic interactions with Phe656 and Tyr652

Table 2. Binding Affinities and Kinetic Parameters of E-4031 Derivatives
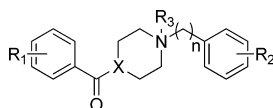
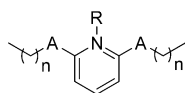| compd	R_1	R_2	X	R_3	n	K_i (nM)	k_{on} (nM^{-1}·min^{-1})	k_{off} (min^{-1})	K_D (nM)	RT (min)
13	4-Cl	3,4-di-Cl	CH		2	54 ± 3	0.021 ± 0.009	0.39 ± 0.06	36 ± 22	2.6 ± 0.4
14	4-CH$_3$	H	CH		3	60 ± 2	0.017 ± 0.003	0.49 ± 0.12	34 ± 14	2.0 ± 0.5
15	H	H	N		2	5418 ± 374	$(2.7 ± 0.6) × 10^{-4}$	0.46 ± 0.03	1812 ± 313	2.2 ± 0.1
16	4-Cl	H	CH	CH$_3$	2	48 ± 1	0.048 ± 0.022	0.35 ± 0.09	18 ± 9	2.9 ± 0.8

Table 3. Binding Affinities and Kinetic Parameters of Clofilium Derivatives
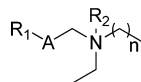
compd	R_1	R_2	A	n	K_i (nM)	k_{on} (nM^{-1}·min^{-1})	k_{off} (min^{-1})	K_D (nM)	RT (min)
17	4-Cl-C$_6$H$_4$CH$_2$		—CH$_2$CH$_2$—	6	31 ± 5	0.048 ± 0.019	0.37 ± 0.04	16 ± 10	2.7 ± 0.3
18	C$_6$H$_5$CH$_2$		–HC:CH–	6	119 ± 2	0.0098 ± 0.0042	0.50 ± 0.12	86 ± 45	2.0 ± 0.5
19	4-CH$_3$-C$_6$H$_5$		—C≡C—	6	3282 ± 613	$(3.2 ± 2.0) × 10^{-4}$	0.13 ± 0.03	1188 ± 122	7.7 ± 1.6
20	4-CH$_3$-C$_6$H$_5$		—C≡C—	2	1196 ± 141	$(3.1 ± 0.7) × 10^{-4}$	0.15 ± 0.05	637 ± 339	6.7 ± 2.0
21	(C$_6$H$_5$)$_2$CH		—C≡C—	6	97 ± 13	0.0035 ± 0.0008	0.27 ± 0.06	100 ± 52	3.7 ± 0.8
22	4-Cl-C$_6$H$_5$	CH$_2$CH$_3$	—C≡C—	6	1.8 ± 0.2	0.17 ± 0.07	0.13 ± 0.04	1.2 ± 0.6	7.7 ± 2.6

Table 4. Binding Affinities and Kinetic Parameters of Pyridinium Analogues[a]

Compd	A	R	n	K_i (nM)	k_{on} (nM^{-1}·min^{-1})	k_{off} (min^{-1})	K_D (nM)	RT (min)
23	—CH$_2$CH$_2$—	-	5	36870±10861	$(2.8±0.4)×10^{-7}$	0.052±0.002	190546±27585	19±1
24	—CH$_2$CH$_2$—	CH$_3$	3	12±1	0.020±0.005	0.23±0.04	12±0	4.3±0.8
25	—CH$_2$CH$_2$—	CH$_3$	4	0.28±0.01	0.25±0.08	0.10 ± 0.02	0.44±0.05	10± 2
26	—CH$_2$CH$_2$—	CH$_3$	5	3.5±0.3	0.023±0.004	0.040±0.002	1.9±0.5	25±1
27	—CH$_2$CH$_2$—	CH$_3$	6	3.4±0.9	0.018±0.003	0.069±0.005	4.0±0.6	14±1
28	—CH$_2$CH$_2$—	CH$_3$	7	17±3	0.0017±0.0002	0.064±0.015	37±5	16±4
29	—CH$_2$CH$_2$—	CH$_3$	9	108±10	$(1.8±0.2)×10^{-4}$	0.028±0.001	153±10	36±2
30	—C≡C—	CH$_3$	9	1179±297	$(3.3±1.1)×10^{-5}$	0.12±0.02	4258±1139	8.3±1.7

Compd	A	R	K_i (nM)	k_{on} (nM^{-1}·min^{-1})	k_{off} (min^{-1})	K_D (nM)	RT (min)
31	—CH$_2$CH$_2$—	-	3654±81	$(1.6±0.3)×10^{-5}$	0.11±0.01	6631±536	9.1±0.8
32	—CH$_2$CH$_2$—	CH$_3$	6.0±0.5	0.022±0.003	0.13±0.01	6.1±1.2	7.7±0.7
33	—C≡C—	CH$_3$	2460±262	$(1.4±0.4)×10^{-5}$	0.11±0.02	8877±1904	9.1±1.7

Compd	R_1	A	R_2	B	K_i (nM)	k_{on} (nM^{-1}·min^{-1})	k_{off} (min^{-1})	K_D (nM)	RT (min)
34	-	—C≡C—	C$_6$H$_5$	C$_6$H$_4$	>100 μM	n.d.	n.d.	n.d.	n.d.
35	CH$_3$	—CH$_2$CH$_2$—	C$_6$H$_5$	C$_6$H$_4$	63±9	0.0016±0.0003	0.098±0.021	60±4	10±2
36	CH$_3$	—C≡C—	H	C$_6$H$_{10}$	1208±36	$(3.3±1.2)×10^{-4}$	0.30±0.05	1074±268	3.3±0.6
37	CH$_3$	—C≡C—	H	C$_6$H$_4$	498±107	0.0086±0.0020	2.9±0.3	368±61	0.34±0.04
38	CH$_3$	—C≡C—	C$_6$H$_5$	C$_6$H$_4$	86±12	$(7.5±1.0) ×10^{-5}$	0.0095±0.0003	132±19	105±4
39	CH$_3$	—C≡C—	2-CH$_3$-C$_6$H$_5$	C$_6$H$_4$	577±41	$(3.5±0.3)×10^{-4}$	0.071±0.004	203±19	14±1
40	CH$_3$	—C≡C—	3-CH$_3$-C$_6$H$_5$	C$_6$H$_4$	122±15	$(1.4±0.2)×10^{-4}$	0.010±0.003	72±18	100±30
41	CH$_3$	—C≡C—	3-OCH$_3$-C$_6$H$_5$	C$_6$H$_4$	176±10	$(3.7±0.4)×10^{-4}$	0.047±0.009	125±13	21± 4
42	CH$_3$	—C≡C—	3-Cl-C$_6$H$_5$	C$_6$H$_4$	139±20	$(8.3±0.9)×10^{-5}$	0.011±0.002	135±14	91±17
43	CH$_3$	—C≡C—	4-CH$_3$-C$_6$H$_5$	C$_6$H$_4$	303±49	$(8.6±1.0)×10^{-5}$	0.033±0.006	440±78	30±6
44	CH$_3$	—C≡C—	4-OCH$_3$-C$_6$H$_5$	C$_6$H$_4$	247±44	$(4.5±0.2)×10^{-4}$	0.042±0.007	105±16	24± 4
45	CH$_3$	—C≡C—	4-OH-C$_6$H$_5$	C$_6$H$_4$	153±32	$(5.1±0.7)×10^{-4}$	0.053±0.008	103±3	19±3
46	CH$_3$	—C≡C—	4-Cl-C$_6$H$_5$	C$_6$H$_4$	71±9	$(1.6±0.2)×10^{-4}$	0.016±0.001	100±10	63±4

[a] n.d.: not detectable.

residues lining the pore cavity of the $K_v11.1$ channel,[36,40] whereby this hindered interaction did not obviously disturb the dissociation of ligands. Overall, the association rates of this series of compounds were (negatively) correlated to their K_i values (see also Figure 3B), which is in full agreement with our previous finding that ligand affinities for the $K_v11.1$ channel are mainly regulated by the compounds' association rates.[2] Unlike the widely varying K_i and k_{on} values, RTs of these dofetilide analogues were largely similar.

Derivatives of E-4031. Benzoylpiperidine analogues (**13**, **14**, and **16**) demonstrated comparable K_i and k_{on} values at the $K_v11.1$ channel. This implicates that (i) electron withdrawing or donating groups at the two peripheral rings, (ii) slightly lengthening the carbon chain between the central nitrogen atom and the phenyl ring, and (iii) permanent protonation of the basic nitrogen had much smaller effects on $K_v11.1$ affinities and association kinetics of E-4031 (N-[4-[1-[2-(6-methylpyridin-2-yl)ethyl]piperidine-4-carbonyl]phenyl]) derivatives (Table 2) compared to the dofetilide series (Table 1). However, when the benzoylpiperidine was replaced by benzoylpiperazine (**15**), the K_i value was drastically increased to 5418 ± 374 nM and its association rate was substantially decreased to $(2.7 \pm 0.6) \times 10^{-4}$ nM^{-1}·min^{-1}. Distinct from the variations in affinities and association rates, all E-4031 derivatives displayed comparably short RTs between 2.0 ± 0.5 (**14**) and 2.9 ± 0.8 min (**16**) at the $K_v11.1$ channel.

Derivatives of Clofilium. Comparable to our own and other studies,[24,25,41] increasing the rigidity by introduction of alkene and alkyne moieties in the chain between the phenyl ring and central nitrogen atom diminished the $K_v11.1$ affinities and association rates of clofilium derivatives (**18** and **21** versus **17**, Table 3), whereby permanent protonation of the central nitrogen atom with a CH_2CH_3 group resulted in a dramatic enhancement of the affinity and association rate ($K_i = 1.8 \pm 0.2$ nM and $k_{on} = 0.17 \pm 0.07$ nM^{-1}·min^{-1} for **22**). Therefore, rigidity and protonation play pivotal roles in determining the affinities and association rates of clofilium analogues at the $K_v11.1$ channel. However, permanently protonating the central nitrogen obviously imposed more significant effects on $K_v11.1$ affinities and association rates and thus compensated for the negative influences exerted by increasing rigidity via introduction of an alkyne bond (**22** versus **17**). According to different in silico $K_v11.1$ models, protonation of the central nitrogen atom facilitates the π−cation interaction of ligands with the crucial binding residue (Tyr652) that faces into the S6 domain of the channel.[36,42−44] With regard to dissociation characteristics, compounds **17** and **18** had similar RTs at the $K_v11.1$ channel (2.7 ± 0.3 and 2.0 ± 0.5 min for **17** and **18**, respectively), while **21** and **22** having an alkyne moiety displayed longer RTs. Subsequently, two novel compounds with an alkyne group but different side chain lengths (**19** and **20**) were synthesized in order to obtain more variations in dissociation rate constants or RTs. Both compounds exhibited comparably low affinities and slow association rates at the $K_v11.1$ channel, indicating the flexibility adjusted by side chain lengths imposed insignificant effects on weakening $K_v11.1$ affinities and association kinetics of this series of ligands. Likewise, the dissociation rates of **19** and **20** were identical with comparatively longer RTs of 7.7 ± 1.6 and 6.7 ± 2.0 min, respectively. Altogether, introduction of an alkyne group in these clofilium analogues slightly increased their RTs at the $K_v11.1$ channel (**19−22** versus **17−18**). With all these clofilium derivatives (Table 3), their association rates illustrated the same overall tendency as the affinities shown in Figure 3B. Most importantly, compound **22** showed the highest affinity, fastest association rate, and longest RT, implying a strong and prolonged inhibition of the $K_v11.1$channel.

Derivatives of Pyridinium. As compounds with high lipophilicity can bind to residue Phe656 of the $K_v11.1$ channel through hydrophobic van der Waals interactions as well, peripheral aromaticity is not essential for their $K_v11.1$ binding.[25,37] In this context, eight aliphatic pyridinium analogues with various side chains (**23−30**) were synthesized or selected to define their SARs and SKRs (Table 4). Several general observations can be made: (i) permanently protonating the central nitrogen atom by a methyl substituent (**23** versus other compounds) and (ii) increasing flexibility via stretching the side alkyl chain from n = 3 to n = 6 (**24** versus **25−27**) enhanced the $K_v11.1$ affinities of compounds. However, the binding affinities were decreased with (iii) the continuous prolongation of side chains up to n = 7 (**24** versus **28−29**) and (iv) replacement of alkane with alkyne (**29** versus **30**). All these results are in excellent agreement with protonation and rigidity rules[45] and with the fact that the large aperture at the bottom of the $K_v11.1$ channel cavity has boundaries that accommodate molecules with defined sizes.[46] Likewise, protonation, flexibility of side chains, and rigidity by an alkyne moiety exerted the same overall effects on association rates of these aliphatic pyridines, which implicates that the affinities of aliphatic pyridinium blockers were correlated to their association rate constants at the $K_v11.1$ channel (see also for dofetilide, E-4031, and clofilium derivatives, Figure 3B). Intriguingly, RTs in this series of compounds tended to be longer and different from the three other compound classes mentioned above as well as from our previous data.[2] The newly synthesized compound **29** had the longest RT of 36 ± 2 min, whereas **24** showed the shortest RT with 4.3 ± 0.8 min. In addition, pyridines with *n*-octyl side chains (**23**, RT = 19 ± 1 min) presented a comparable RT to **26** (25 ± 1 min) and **28** (16 ± 4 min) at the $K_v11.1$ channel. Apparently, permanent protonation of the central nitrogen atom (**23** versus **26**) and prolongation of side alkyl chains (**28** versus **23** and **26**) had much less influence on RTs compared to their roles in overall affinities and association rates. It is noteworthy that more rigidity induced by an alkyne moiety diminished the RT to 8.3 ± 1.7 min for **30**. Altogether, increasing rigidity of aliphatic pyridine blockers can decrease their affinities, association rates, and RTs simultaneously (**30** versus **29**), and thus it may provide an efficient solution for circumventing $K_v11.1$ side effects of drug candidates. In a second series of pyridinium analogues (**31−33**), the $K_v11.1$ affinities and association rates were also increased by permanent protonation of the central nitrogen atom (**32** versus **31**) but decreased with an alkyne moiety (**33** versus **32**). However, the RTs of **31−33** were comparable between 7.7 ± 0.7 (**32**) and 9.1 ± 1.7 min (**33**), indicating different dissociation profiles of these compounds compared to aliphatic pyridinium analogues of which rigidity affected the RTs significantly.

Next, a series of biphenyl substituted pyridinium derivatives (**34**, **35**, and **38−46**) together with their precursors (**36** and **37**) were synthesized or selected to achieve more variations in RTs. As shown in Table 4, permanent protonation and rigidification by alkyne imposed the same effects on $K_v11.1$ affinities as our findings for other derivatives (**34** versus **35−46** and **35** versus **36−46**, respectively). Additionally, decreasing bulkiness via removal of the second benzene rings or replacing the aromatic phenyl rings close to the central nitrogen atom

with cyclohexyl diminished the affinities of $K_v11.1$ blockers (**36**−**37** versus **38**), possibly caused by reduced π-stacking and hydrophobic interactions.[36] Furthermore, introduction of different groups at the second benzene rings lowered their $K_v11.1$ affinities compared to the nonsubstituted compound (**39**−**45** versus **38**), indicating a possible steric hindrance of these groups in ligand binding.[22,25] Although the k_{on} values showed a comparable decline to affinities because of the increased rigidity by an alkyne moiety (**35** versus **38**−**46**) and reduction of the aromatic rings (**36** versus **37**), the negative relationship between K_i and k_{on} values was not conspicuous for this series of compounds. For instance, compound **38** showed a smaller K_i value as well as slower association rate than **39**. On the contrary, the RTs of these compounds were significantly increased by replacing ethyl with alkyne (**35** versus **38**−**46**). Moreover, decreasing bulkiness of these pyridinium analogues led to shorter RTs (**36**−**37** versus **38**−**46**). Compound **36** and **37** showed the shortest RTs among all these derivatives, providing evidence that reduced bulkiness facilitates unbinding dynamics of $K_v11.1$ blockers at the channel. Our findings are contradictory to the classic "foot-in-door" mechanism, in which bulky residues of $K_v11.1$ blockers prevent the closure of the channel gate and thus promote the channel recovery from blockade.[20] The explanation for our results is that less hydrophobic interactions and smaller sizes of molecules can accelerate the dissociation of such ligands from the channel. Compound **38** without any substituents on the benzene rings had the longest RT of 105 ± 4 min at the $K_v11.1$ channel, while substituents at the second benzene rings (**39**−**46**) often had distinct and lowering effects on RTs. While introducing CH_3 (**40**) and Cl (**42**) at the meta-position did not affect RTs significantly, a substituent at the ortho-position (**39**) of the benzene rings reduced the RT, like at the para-position (**43**−**46**) but to a lesser extent (**43** versus **39**). Second, a methoxy group at the meta-position of the second benzene rings was less favorable for maintaining long RTs (**41** versus **40** and **42**). A similar observation was made for the two compounds with 4-OCH_3 (**44**) and 4-OH (**45**) groups at the second benzene rings, of which RTs were decreased to 24 ± 4 and 19 ± 3 min, respectively, particularly when compared with **46** (63 ± 4 min) and **43** (30 ± 6 min). Collectively, we have successfully obtained compounds with divergent RTs (i.e., approximately 300-fold difference, between **37** and **38**) next to varied affinities and association rates, which provides the possibility to investigate the influence of RTs on in vivo cardiotoxicity of $K_v11.1$ blockers.

Kinetic Map. Using the kinetic data in Tables 1−4, we plotted the dissociation rates (pk_{off}, y axis) against association rates (pk_{on}, x axis) of all our compounds together with three reference compounds (astemizole, dofetilide, and ranolazine) into a kinetic map (Figure 4). The parallel diagonal dashed lines represent the kinetically derived K_D values. In this k_{on}−k_{off}−K_D map, compounds with the same affinities or association rates may have divergent dissociation rates, or RTs, and vice versa. Therefore, risk assessment and possible mitigation of inhibitory efficacies of $K_v11.1$ blockers should take association rates (k_{on}) and RTs into account rather than affinities alone. In this context, all ligands were divided into four quadrants (**I**, **II**, **III**, and **IV**) according to our hypothesis that high affinities, fast association rates, and slow dissociation rates (long RTs) contribute together to serious $K_v11.1$-induced cardiotoxicity. The affinities and kinetic parameters of astemizole, dofetilide, and ranolazine were derived from our previous investigation.[2]

Astemizole was distributed into quadrant **II**, as it is a specific $K_v11.1$ blocker and has been withdrawn from the market.[26,27] On the other hand, ranolazine was assigned to quadrant **IV** because it inhibits the $K_v11.1$ channel but does not cause pro-arrhythmic events.[28] Dofetilide's use is restricted in the United States due to the compound causing TdP by blocking the $K_v11.1$ channel,[27,47,48] and consequently, it was brought into quadrant **III**. Obviously, compounds in quadrant **II** have high affinities ($K_D < 316$ nM), fast association rates ($k_{on} > 3.2 \times 10^{-4}$ $nM^{-1} \cdot min^{-1}$), and slow dissociation rates or long RTs (>10 min) at the $K_v11.1$ channel, indicating that they may cause serious arrhythmias via blockade of the channel. On the other hand, quadrant **IV** comprises compounds with low affinities ($K_D > 316$ nM), slow association rates ($k_{on} < 3.2 \times 10^{-4}$ $nM^{-1} \cdot min^{-1}$), and fast dissociation rates or short RTs (<10 min) at the channel, suggesting their possible cardiac safety in terms of $K_v11.1$ inhibition. Quadrants **I** and **III** encompass moderately active $K_v11.1$ blockers with either relatively low affinities, slow k_{on} (<3.2×10^{-4} $nM^{-1} \cdot min^{-1}$) and k_{off} (RT > 10 min, **I**), or comparatively high affinities, fast k_{on} (>3.2×10^{-4} $nM^{-1} \cdot min^{-1}$), and k_{off} (RT < 10 min, **III**). Most likely these two different classes of compounds have modest $K_v11.1$-related cardiac side effects. Taken together, this provisional kinetic map that can be further extended with other suspected $K_v11.1$ blockers sheds light on $K_v11.1$-induced cardiotoxicity of drugs by bringing together their affinities as the traditional safety parameter with their kinetic parameters of association and dissociation rates (or RTs) at the channel. Therefore, a similar map would provide valuable information on how to accurately and comprehensively evaluate and further circumvent $K_v11.1$ liabilities of drug candidates in the future.

Patch Clamp Study. A whole-cell voltage patch clamp assay was applied to determine the functional hERG current blockade by **21** and **38**, two compounds with similar affinities but different RTs. As shown in Figure 5A, the IC_{50} values for **21** and **38** from their concentration−effect curves in the patch clamp assay were 182 ± 6 and 107 ± 6 nM, respectively. However, **21** and **38** had almost identical affinities in the radioligand binding assay with K_i values of 97 ± 13 and 86 ± 12 nM, respectively. RTs of ligands have been found to be correlated to their efficacies in functional assays rather than affinities at the adenosine A_{2A} receptor.[49] Thus, we surmised that the difference in IC_{50} values obtained in functional patch clamp assays for these two compounds might be caused by their different RTs, with **38** (long RT of 105 ± 4 min) displaying a higher potency in $K_v11.1$ current inhibition than **21** (short RT of 3.7 ± 0.8 min). The time-dependent inhibition of the $K_v11.1$ current for **21** and **38** was also assessed in the whole-cell patch clamp assay. As shown in Figure 5B, compound **21** with a faster association rate (0.0035 ± 0.0008 $nM^{-1} \cdot min^{-1}$) in the radioligand binding assay almost completely inhibited $K_v11.1$ currents within 10 min, whereas 15 min was required for **38** ($k_{on} = (7.5 \pm 1.0) \times 10^{-5}$ $nM^{-1} \cdot min^{-1}$) to approach the equilibrated current inhibition. Therefore, association rates measured in the [^{3}H]dofetilide competition association assay may be linked to the current inhibition rates of compounds in the functional patch clamp experiments. Although different wash-in times for $K_v11.1$ blockers have been observed on an automated patch clamp platform before,[23] this is the first time to interpolate the radioligand binding parameters, especially for the association and dissociation rates, into functional data derived from patch clamp assays.

CONCLUSION

Although affinities and association rates of compounds at the $K_v11.1$ channel have been found to differ vastly and are correlated to each other, this study is the first to verify that $K_v11.1$ blockers can possess very different RTs, with up to a more than 300-fold difference (**37** versus **38**) at the channel. Furthermore, this comprehensive investigation on derivatives of dofetilide, E-4031, clofilium, and pyridinium over a range of scaffolds is the first to illustrate the impact of several parameters outlined above on association rates and RTs of compounds at the $K_v11.1$ channel in addition to their binding affinities. Notably, unlike the consistency of SARs for all compounds, SKRs are more chemical scaffold-dependent, in particular the structure−RT relationships. According to these findings and helped by the substantial differences in affinities, association and dissociation rate constants, or RTs in the current sets of compounds, we delineated a $k_{on}−k_{off}−K_D$ kinetic map and divided all these compounds into four quadrants (toxic for quadrant **II**, safe for quadrant **IV**, and suspicious for quadrant **I** and **III** in Figure 4), which might provide valuable information for pharmaceutical researchers to devise better strategies for assessing $K_v11.1$ liabilities. Additionally, the association rates of two selected compounds (**21** and **38**) were found to correspond well with their current block rates in the patch clamp studies, and their distinct RTs are a possible reason for their differences in functional potencies when compared to their binding affinities. Although far from complete, this analysis further indicates that kinetic parameters (k_{on} and RTs) as well as affinities (K_i) should be taken into consideration during the investigation of $K_v11.1$-mediated adverse reactions. To conclude, the new finding of large variations in RTs promotes the extensive analysis of structure−RT relationships, and the combination of SARs and SKRs opens a new avenue for medicinal chemists to more efficiently design new chemical entities with low or negligible $K_v11.1$-induced cardiotoxicity.

EXPERIMENTAL SECTION

Chemistry. All commercially available chemicals and solvents were used without purification, except for ethyl acetate, which was distilled before usage. Demineralized water will be referred to as H_2O unless otherwise stated. Reactions were monitored by thin-layer chromatography (TLC) using TLC silica gel 60 F254 aluminum sheets. TLC visualization was performed by a LAMAG UV-light at a wavelength of 254 or 366 nm. Grace Davison Davisil silica column material (LC60A 30−200 μm) was used for purification by column chromatography. ^1H and ^{13}C NMR spectra were recorded on a Bruker AV400 or AV600 spectrometer. Deuterated solutions $CDCl_3$, DMSO, or MeOD were used for sample preparation. Chemical shifts (δ) are given in ppm and coupling constants (J) in hertz. Trimethylsilane was used as internal standard for calibrating chemical shift for ^1H and ^{13}C NMR spectroscopy. HPLC- analysis was carried out on a Phenomenex Gemini reversed-phase C18 column (50 mm × 4.6 mm × 3 μm) coupled to a UV detector at 254 nm. Final compounds were dissolved in either a mixture of acetonitrile:*tert*-butanol:water (1:1:1) or in pure acetonitrile and were eluted from the column at a flow rate of 1.30 mL· min^{-1} with 10/90 acetonitrile/water +10% TFA, decreasing polarity of this mixture in time. LC-MS analysis was performed on an LCQ Advantage Max (Thermo Finnigan) ion-trap spectrometer (ESI$^+$) coupled to a Surveyor HPLC system (Thermo Finnigan) equipped with a C18 column (Phenomenex Gemini, 50 mm × 4.6 mm, 5 μm). A linear gradient of 10/90 acetonitrile/water + a constant 10% of an 1% TFA in water solution was used as the mobile system. The purity of all final compounds was >95%. High-resolution mass spectral analysis (HRMS) was performed by Leiden Institute of Chemistry by direct injection (2 μL of a 2 μM solution in water/MeCN; 50/50; v/v and 0.1% formic acid) on a LTQ-Orbitrap FTMS operated in a positive ionization mode with an electrospray ionization (ESI) source (source voltage 3.5 kV, sheath gas flow 10%, capillary temperature 275 °C) with resolution $R = 60000$ at m/z 400 (mass range $m/z = 150−2000$) and calibrated for dioctyl phthalate ($m/z = 391.28428$). All microwave reactions were performed in a Biotage initiator 2.5 in a sealed microwave vial.

N-Ethyl-N-(3-(p-tolyl)prop-2-yn-1-yl)heptan-1-amine (19). To a solution of **S14** (300 mg, 1 mmol) in DMF (5 mL) was added K_2CO_3 (415 mg, 3 mmol) followed by N-ethylheptylamine (280 μL, 1.5 mmol). The mixture was stirred at rt for 1 h and diluted with water (5 mL) and extracted with EtOAc (3 × 10 mL), and the organic layers were dried on $MgSO_4$ and filtered, and the solvent was removed in vacuo. The crude residue was purified by flash chromatography on silica gel (20% EtOAc−petroleum ether) to afford pure **19** as an oil. Yield (228 mg) 84%. ^1H NMR (400 MHz, $CDCl_3$) δ 7.32 (d, $J = 8.0$ Hz, 2H), 7.10 (d, $J = 8.0$ Hz, 2H), 3.62 (s, 2H), 2.61 (q, $J = 7.2$ Hz, 2H), 2.53 (t, $J = 7.6$ Hz, 2H), 2.34 (s, 3H), 1.52−1.49 (m, 2H), 1.31−1.26 (m, 8H), 1.11 (t, $J = 7.2$ Hz, 3H), 0.88 (t, $J = 7.2$ Hz, 3H) ppm. ^{13}C NMR (101 MHz, $CDCl_3$) δ 137.9, 131.6, 129.0, 120.3, 85.0, 83.8, 53.6, 47.7, 42.1, 31.9, 29.3, 27.6, 27.5, 22.7, 21.4, 14.1, 12.7 ppm. HPLC: $t_R = 7.39$ min. HRMS (ESI): m/z $[M + H]^+$ calcd for $C_{19}H_{29}N$, 272.2373; found, 272.2370.

N-Ethyl-N-propyl-3-(p-tolyl)prop-2-yn-1-amine (20). To a solution of **S14** (300 mg, 1 mmol) in DMF (5 mL) was added K_2CO_3 (415 mg, 3 mmol) followed by N-ethylpropylamine (180 μL, 1.5 mmol). The mixture was stirred at rt for 1 h and diluted with water (5 mL) and extracted with EtOAc (3 × 10 mL), and the organic layers were dried on $MgSO_4$ and filtered, and the solvent was removed in vacuo. The crude residue was purified by flash chromatography on silica gel (20% EtOAc−petroleum ether) to afford pure **20** as oil. Yield (170 mg) 79%. ^1H NMR (400 MHz, $CDCl_3$) δ 7.32 (d, $J = 8.0$ Hz, 2H), 7.10 (d, $J = 8.0$ Hz, 2H), 3.62 (s, 2H), 2.61 (q, $J = 7.2$ Hz, 2H), 2.50 (t, $J = 7.6$ Hz, 2H), 2.34 (s, 3H), 1.53 (sex, $J = 7.6$ Hz, 2H), 1.11 (t, $J = 7.2$ Hz, 3H), 0.93 (t, $J = 7.6$ Hz, 3H) ppm. ^{13}C NMR (101 MHz, $CDCl_3$) δ 137.9, 131.6, 129.0, 120.3, 85.0, 83.8, 55.6, 47.6, 42.1, 21.4, 20.8, 12.7, 12.0 ppm. HPLC: $t_R = 5.70$ min. HRMS (ESI): m/z $[M + H]^+$ calcd for $C_{15}H_{21}$, 216.1747; found, 216.1745.

General Methylation Procedure to Yield Pyridines 24, 25, 27−30, 39−44, and 46. The respective compound **S23e**, **S24a−e**, **S34a−e**, **S46**, and **S47** (1.0 equiv) was dissolved in CH_2Cl_2 (40 mL per mmol) and stirred at 0 °C under a N_2 atmosphere. Methyl trifluoromethanesulfonate (2.8 equiv) was added, and the mixture was stirred overnight. After adsorption of the crude on silica, FCC gave the desired compound eluting with a mixture of dichloromethane:methanol.

2,6-Dihexyl-1-methylpyridinium Trifluoromethanesulfonate (24). Prepared from **S24a** and purified by FCC (dichloromethane:methanol 60:1 to 20:1) to give the desired product. Yield (660 mg) 85%. ^1H NMR (400 MHz, $CDCl_3$): δ 8.20 (t, $J = 8.0$ Hz, 1H), 7.64 (d, $J = 8.0$ Hz, 2H), 4.21 (s, 3H), 3.12 (t, $J = 7.6$ Hz, 4H), 1.81−1.74 (m, 4H),), 1.52−1.45 (m, 4H), 1.39−1.29 (m, 8H), 0.91 (t, $J = 6.8$ Hz, 6H). ^{13}C NMR (101 MHz, $CDCl_3$): δ 159.7, 144.2, 126.0, 39.7, 34.5, 31.4, 28.9, 27.6, 22.5, 14.1 ppm. HPLC purity: 99.3% (t_R 8.24 min). ESI-MS: 262.27 [M].

2,6-Diheptyl-1-methylpyridinium Trifluoromethanesulfonate (25). Prepared from **S24b** and purified by FCC (dichloromethane:methanol 30:1 to 20:1) to give the desired product. Yield (143 mg) 86%. ^1H NMR (400 MHz, $CDCl_3$): δ 8.18 (t, $J = 7.6$ Hz, 1H), 7.63 (d, $J = 8.0$ Hz, d), 4.22 (s, 3H), 3.13 (t, $J = 8.0$ Hz, 4H), 1.82−1.74 (m, 4H), 1.52−1.44 (m, 4H), 1.41−1.36 (m, 12H), 0.90 (t, $J = 6.4$ Hz, 6H). ^{13}C NMR (101 MHz, $CDCl_3$): δ 159.8, 144.1, 126.0, 122.4, 119.2, 39.7, 34.6, 31.7, 29.3, 29.0, 27.7, 22.7, 14.2 ppm. HPLC purity: 97% (t_R 8.96 min). ESI-MS: 290.33 [M].

2,6-Dinonyl-1-methylpyridinium Trifluoromethanesulfonate (27). Prepared from **S24c** and purified by FCC (dichloromethane:methanol 30:1 to 15:1) to give the desired product. Yield (87 mg) 65%. ^1H NMR (400 MHz, $CDCl_3$): δ 8.18 (t, $J = 8.0$ Hz, 1H), 7.63 (d, $J = 8.0$ Hz, 2H), 4.22 (s, 3H), 3.12 (t, $J = 7.6$ Hz, 4H), 1.82−1.74 (m,

4H), 1.50−1.46 (m, 4H), 1.44−1.28 (m, 20H), 0.89 (t, J = 6.4 Hz, 6H). ^{13}C NMR (101 MHz, CDCl$_3$): δ 159.9, 144.0, 126.0, 39.8, 34.6, 32.0, 29.5, 29.4, 27.7, 22.8, 14.2 ppm. HPLC purity: 100% (t_R 10.21 min). ESI-MS: 346.40 [M].

2,6-Didecyl-1-methylpyridinium Trifluoromethanesulfonate (28). Prepared from S24d and purified by FCC (dichloromethane:methanol 60:1 to 10:1) to give the desired product. Yield (166 mg) 74%. ^{1}H NMR (400 MHz, CDCl$_3$): δ 8.18 (t, J = 8.0 Hz, 1H), 7.63 (d, J = 8.0 Hz, 2H), 4.22 (s, 3H), 3.13 (t, J = 8.0 Hz, 4H), 1.82−1.74 (m, 4H), 1.50−1.44 (m, 4H), 1.39−1.28 (m, 24H), 0.89 (t, J = 6.8 Hz, 6H). ^{13}C NMR (101 MHz, CDCl$_3$): δ 159.7, 144.0, 125.9, 39.6, 34.4, 31.9, 29.5, 29.4, 29.3, 29.2, 27.6, 22.7, 14.1 ppm. HPLC purity: 100% (t_R 10.77 min). ESI-MS: 374.40 [M].

2,6-Didodecyl-1-methylpyridinium Trifluoromethanesulfonate (29). Prepared from S24e and purified by FCC (dichloromethane:methanol 30:1 to 20:1) to give the desired product. Yield (536 mg) 87%. ^{1}H NMR (400 MHz, CDCl$_3$): δ 8.19 (t, J = 8.0 Hz, 1H), 7.63 (d, J = 7.6 Hz, 2H), 4.21 (s, 3H), 3.12 (t, J = 8.0 Hz, 4H), 1.81−1.73 (m, 4H), 1.51−1.44 (m, 4H), 1.38−1.27 (m, 32H), 0.88 (t, J = 6.8 Hz, 6H). ^{13}C NMR (101 MHz, CDCl$_3$): δ 159.8, 144.1, 126.0, 39.7, 34.6, 32.0, 29.8, 29.7, 29.7, 29.6, 29.5, 29.4, 29.3, 27.7, 22.8, 14.2 ppm. HPLC purity: 100% (t_R 11.84 min). ESI-MS: 430.53 [M].

2,6-Di(dodec-1-ynyl)-1-methylpyridinium Trifluoromethanesulfonate (30). Prepared from S23e and purified by FCC (dichloromethane:methanol 40:1 to 20:1) to give the desired product. Yield (675 mg) 94%. ^{1}H NMR (400 MHz, CDCl$_3$): δ 8.38 (t, J = 8.0 Hz, 1H), 7.90 (d, J = 8.0 Hz, 2H), 4.49 (s, 3H), 2.65 (t, J = 7.2 Hz, 4H), 1.74−1.65 (m, 4H), 1.48−1.41 (m, 4H), 1.30−1.27 (m, 24H), 0.88 (t, J = 6.8 Hz, 6H). ^{13}C NMR (101 MHz, CDCl$_3$): δ 144.3, 139.5, 130.7, 112.8, 72.9, 45.1, 32.0, 29.7, 29.5, 29.4, 29.2, 29.1, 27.6, 22.9, 20.3, 14.2 ppm. HPLC purity: 100% (t_R 11.57 min). ESI-MS: 422.40 [M].

2,6-Di([4-(2-methylphenyl)phenyl]ethynyl)-1-methylpyridinium Trifluoromethanesulfonate (39). Prepared from S34a and purified by FCC (dichloromethane:methanol 30:1 to 20:1) and preparative HPLC to give the desired product. Yield (1 mg) 96%. ^{1}H NMR (400 MHz, CDCl$_3$): δ 8.47 (t, J = 8.0 Hz, 1H), 8.10 (d, J = 8.0 Hz, 2H), 7.77 (d, J = 8.0 Hz, 4H), 7.46 (d, J = 8.0 Hz, 4H), 7.31−7.09 (m, 8H), 4.74 (s, 3H), 2.30 (s, 6H). HPLC purity: 96% (t_R 9.97 min). ESI-MS: 474.33 [M].

2,6-Di([4-(3-methylphenyl)phenyl]ethynyl)-1-methylpyridinium Trifluoromethanesulfonate (40). Prepared from S34b and purified by FCC (dichloromethane:methanol 30:1 to 20:1) to give the desired product. Yield (18 mg) 78%. ^{1}H NMR (400 MHz, CDCl$_3$): δ 8.40 (t, J = 8.0 Hz, 1H), 8.03 (d, J = 8.0 Hz, 2H), 7.73 (d, J = 8.0 Hz, 4H), 7.65 (d, J = 8.0 Hz, 4H), 7.41−7.37 (m, 4H), 7.35 (t, J = 7.6 Hz, 2H), 7.22 (d, J = 7.2 Hz, 2H), 4.65 (s, 3H), 2.41 (s, 6H). ^{13}C NMR (101 MHz, CDCl$_3$): δ 145.0, 143.9, 139.5, 138.9, 133.5, 129.4, 129.1, 128.1, 127.7, 124.4, 117.5, 109.0, 81.2, 45.5, 21.7 ppm. HPLC purity: 98.65% (t_R 10.24 min). ESI-MS: 474.33 [M].

2,6-Di([4-(3-methoxyphenyl)phenyl]ethynyl)-1-methylpyridinium Trifluoromethanesulfonate (41). Prepared from S46 and purified by FCC (dichloromethane:methanol 20:1 to 10:1) to give the desired product. Yield (12 mg) 36%. ^{1}H NMR (400 MHz, CDCl$_3$): δ 8.39 (t, J = 8.0 Hz, 1H), 8.02 (d, J = 8.0 Hz, 2H), 7.73 (d, J = 8.0 Hz, 4H), 7.65 (d, J = 8.4 Hz, 4H), 7.37 (t, J = 7.6 Hz, 2H), 7.18 (d, J = 8.0 Hz, 2H), 7.11 (s, 2H), 6.94 (dd, J_1 = 8.2 Hz, J_2 = 2.0 Hz, 2H), 4.63 (s, 3H), 3.86 (s, 6H). ^{13}C NMR (101 MHz, CDCl$_3$): 160.3, 144.6, 143.9, 140.9, 139.3, 133.5, 130.8, 130.3, 127.7, 119.7, 117.7, 114.0, 113.0, 108.8, 81.3, 55.5, 45.5, 29.9 ppm. HPLC purity: 99% (t_R 9.56 min). ESI-MS: 506.33 [M].

2,6-Di([4-(3-chlorophenyl)phenyl]ethynyl)-1-methylpyridinium Trifluoromethanesulfonate (42). Prepared from S47 and purified by FCC (dichloromethane:methanol 20:1 to 10:1) to give the desired product. Yield (9 mg) 45%. ^{1}H NMR (400 MHz, CDCl$_3$): δ 8.43 (t, J = 8.0 Hz, 1H), 8.08 (d, J = 8.0 Hz, 2H), 7.78 (d, J = 8.0 Hz, 4H), 7.65 (d, J = 8.0 Hz, 4H), 7.57 (s, 2H), 7.48 (d, J = 7.2 Hz, 2H), 7.42−7.37 (m, 4H), 4.70 (s, 3H). ^{13}C NMR (101 MHz, CDCl$_3$/MeOD): δ 143.8, 143.4, 141.0, 139.3, 134.9, 133.3, 130.7, 130.3, 128.5, 127.6, 127.1, 125.3, 117.9, 108.5, 80.8, 45.0, 29.5 ppm. HPLC purity: 99% (t_R 10.20 min). ESI-MS: 514.33 [M].

2,6-Di(4-(4-methylphenyl)phenylethynyl)-1-methylpyridinium Trifluoromethanesulfonate (43). Prepared from S34c and purified by FCC (dichloromethane:methanol 30:1 to 5:1) to give the desired product. Yield (27 mg) 48%. ^{1}H NMR (400 MHz, CDCl$_3$): δ 8.43 (t, J = 8.0 Hz, 1H), 8.06 (d, J = 8.0 Hz, 2H), 7.75 (d, J = 8.4 Hz, 4H), 7.67 (d, J = 8.4 Hz, 4H), 7.52 (d, J = 8.0 Hz, 4H), 7.29−7.26 (m, 4H), 4.68 (s, 3H), 2.41 (s, 6H). ^{13}C NMR (101 MHz, CDCl$_3$/MeOD): δ 144.9, 143.9, 139.4, 138.8, 136.3, 133.4, 133.3, 130.6, 129.8, 127.4, 127.0, 117.0, 109.1, 80.9, 77.3, 21.1 ppm. HPLC purity: 99% (t_R 10.28 min). ESI-MS: 474.40 [M].

2,6-Di([4-(4-methoxyphenyl)phenyl]ethynyl)-1-methylpyridinium Trifluoromethanesulfonate (44). Prepared from S34d and purified by FCC (dichloromethane:methanol 30:1 to 10:1) to give the desired product. Yield (42 mg) 58%. ^{1}H NMR (400 MHz, CDCl$_3$): δ 8.42 (t, J = 8.0 Hz, 1H), 8.04 (d, J = 8.0 Hz, 2H), 7.73 (d, J = 8.4 Hz, 4H), 7.65 (d, J = 8.4 Hz, 4H), 7.57 (d, J = 8.8 Hz, 4H), 7.00 (d, J = 8.8 Hz, 4H), 4.67 (s, 3H), 3.86 (s, 6H). ^{13}C NMR (101 MHz, CDCl$_3$/MeOD): δ 160.1, 144.5, 143.7, 139.3, 133.3, 131.6, 130.4, 128.3, 127.0, 116.5, 114.5, 109.3, 80.7, 55.4, 44.9 ppm. HPLC purity: 100% (t_R 9.78 min). ESI-MS: 506.33 [M].

2,6-Di([4-(4-hydroxyphenyl)phenyl]ethynyl)-1-methylpyridinium Trifluoromethanesulfonate (45). 44 (27 mg, 0.04 mmol) was dissolved in 2 mL of CH$_2$Cl$_2$ and cooled to −78 °C under a nitrogen atmosphere. An 1 M solution of BBr$_3$ in CH$_2$Cl$_2$ (0.4 mL) was added and the reaction mixture was allowed to warm up to room temperature and stirring was continued for 2 h at room temperature, after which as shown by TLC (dichloromethane:methanol 30:1) full conversion was reached. The reaction mixture was recooled to −78 °C and quenched with H$_2$O. After an hour, the precipitate was filtered off and washed with H$_2$O and CH$_2$Cl$_2$, respectively, and dried in vacuo. Yield (12 mg) 48%. ^{1}H NMR (400 MHz, DMSO): δ 9.81 (s, 2H), 8.56 (t, J = 8.4 Hz, 1H), 8.36 (d, J = 7.6 Hz, 2H), 7.89 (d, J = 8.0 Hz, 4H), 7.83 (d, J = 8.4 Hz, 4H), 7.64 (d, J = 8.4 Hz, 4H), 6.90 (d, J = 8.8 Hz, 4H), 4.58 (s, 3H). ^{13}C NMR (151 MHz, DMSO): δ 158.2, 143.6, 143.2, 133.3, 130.6, 129.1, 128.2, 126.3, 116.4, 115.9, 106.0, 81.7, 45.2 ppm. HPLC purity 99% (t_R 8.38 min). ESI-MS: 478.33 [M].

2,6-Di([4-(4-chlorophenyl)phenyl]ethynyl)-1-methylpyridinium Trifluoromethanesulfonate (46). Prepared from S34e and purified by FCC (dichloromethane:methanol 30:1 to 10:1) to give the desired product. Yield (42 mg) 58%. ^{1}H NMR (400 MHz, CDCl$_3$): δ 8.43 (t, J = 8.0 Hz, 1H), 8.08 (d, J = 8.4 Hz, 2H), 7.79 (d, J = 8.4 Hz, 4H), 7.67 (d, J = 8.4 Hz, 4H), 7.56 (d, J = 8.4 Hz, 4H), 7.46 (d, J = 8.4 Hz, 4H), 4.74 (s, 3H). ^{13}C NMR (101 MHz, CDCl$_3$/MeOD): δ 143.8, 143.6, 139.3, 137.7, 134.8, 133.4, 130.6, 129.2, 128.4, 127.4, 117.6, 108.6, 80.9, 45.0 ppm. HPLC purity: 99% (t_R 10.39 min). ESI-MS: 514.27 [M].

Biology. *Chemical and Reagents.* [3H]Dofetilide (specific activity 82.3 Ci·mmol^{-1}) was purchased from PerkinElmer (Groningen, The Netherlands). Astemizole was purchased from Sigma-Aldrich (Zwijndrecht, The Netherlands). Bovine serum albumin (BSA, fraction V) was purchased from Sigma (St. Louis, MO, USA). G418 was obtained from Stratagene (Cedar Creek, USA). All the other chemicals were of analytical grade and purchased from standard commercial sources. Human embryonic kidney cells stably expressing the K$_v$11.1 channel (HEK293 K$_v$11.1) were kindly provided by Dr Eckhard Ficker (University of Cleveland, USA).

Cell Culture and Membrane Preparation. HEK293 K$_v$11.1 cells were cultured and membranes were prepared and stored as described previously.[50]

Radioligand Displacement Assay. The binding affinities of all tested compounds was evaluated at 25 °C in a [3H]dofetilide competitive displacement assay as reported earlier.[2]

Radioligand Competition Association Assay. The binding kinetics of unlabeled compounds were determined at 25 °C using a [3H]dofetilide competition association assay as described before,[2] and the concentrations of unlabeled compounds used in this assay were equivalent to their IC$_{50}$ values.

Patch Clamp Assay. HEK293 K$_v$11.1 cells were cultured on 10 mm glass coverslips and placed in a perfusion chamber (Cell Micro-controls, Norfolk, USA) at room temperature and perfused with

control or test solutions. Whole cell patch clamp measurements and data acquisition were performed using an Axopatch-200B amplifier controlled by the pClamp software package version 10 (Axon Instruments, Foster City, CA). Patch pipettes were made with a Sutter P-2000 micropipette puller (Sutter Instrument Company, Novato, USA) and had resistances of 1.5–2.5 MΩ after having been fire polished and filled with pipet solution. Control bath perfusion solution contained (mM): 140 NaCl, 4 KCl, 10 HEPES, 2 $CaCl_2$, 1 $MgCl_2$ (pH 7.2, NaOH), and the pipet filling solution consisted of (mM): 10 KCl, 125 K-gluconate, 0.6 $CaCl_2$, 2 $MgCl_2$, 5 HEPES, 4 Na_2ATP, 5 EGTA (pH 7.2, KOH). After establishing the whole cell configuration, capacitive transients and pipet access resistance were compensated for by 80%.

The pulse protocol for whole cell voltage clamp measurements of $K_v11.1$-mediated ion currents was as follows. Cells were depolarized to 20 mV from a holding potential −80 mV for 4000 ms, allowing a step current due to activation and inactivation of the $K_v11.1$ channels. This was followed by repolarization to a test potential of −50 mV for 5000 ms, during which a tail current was induced by the fast recovery from inactivation and slow deactivation of the channels. The peak tail currents were used for data analysis, and current inhibition was derived from dividing the mean tail current in the presence of selected compounds by the mean tail current under control conditions. Concentration-dependent effects of compounds **21** and **38** on $K_v11.1$ currents were tested at five different concentrations with an equilibrium time of 6.5 min for each concentration in a perfusion system. To determine time-dependent effects, wash-in experiments were performed with a perfusion of bath solution containing 1 μM **21** or **38**. Clampfit 10.4 (Axon Instruments, Foster City, CA) and Prism v. 5.1 (GraphPad, San Diego, CA, USA) were used in analyzing, processing, and plotting the data.

Data Analysis. All experimental data were analyzed using the nonlinear regression curve fitting program Prism v. 5.1 (GraphPad, San Diego, CA, USA). Apparent inhibitory binding constants (K_i values) were derived from the IC_{50} values according to the Cheng–Prusoff equation with the K_D value obtained from saturation assay.[2,35] Association and dissociation rates for unlabeled compounds were calculated by fitting the data into the competition association model using "kinetics of competitive binding":[34]

$$K_A = k_1[L] + k_2$$

$$K_B = k_3[I] + k_4$$

$$S = \sqrt{(K_A - K_B)^2 + 4k_1k_3LI10^{-18}}$$

$$K_F = 0.5(K_A + K_B + S)$$

$$K_S = 0.5(K_A + K_B - S)$$

$$Q = \frac{B_{max}k_1L10^{-9}}{K_F - K_S}$$

$$Y = Q\left(\frac{k_4(K_F - K_S)}{K_F K_S} + \frac{k_4 - K_F}{K_F}e^{(-K_F X)} - \frac{k_4 - K_S}{K_S}e^{(-K_S X)}\right)$$

Where X is the time (min), Y the specific binding of [³H]dofetilide, k_1 and k_2 are the k_{on} ($M^{-1} min^{-1}$) and k_{off} (min^{-1}) of [³H]dofetilide, L the concentration of [³H]dofetilide (nM), B_{max} the maximum specific binding (dpm), and I the concentration of the unlabeled compound (nM). Fixing these parameters allowed the following parameters to be calculated: k_3, which is the k_{on} value ($M^{-1} min^{-1}$) of the unlabeled compound, and k_4, which is the k_{off} value (min^{-1}) of the unlabeled compound. The association and dissociation rates were used to calculate the kinetic K_D values from the following equation: $K_D = k_{off}/k_{on}$. The residence time (RT) was calculated according to the formula: RT = $1/k_{off}$. All values in this study are means of at least three independent experiments with SEM.

ASSOCIATED CONTENT

Ⓢ Supporting Information

Full experimental procedures for synthesis of intermediate compounds **S13**, **S14**, **S23a−e**, **S24a−e**, **S32**, **S33**, **S34a−e**, **S43a**, **S43b**, **S44a**, **S44b**, and **S45−47** including NMR data (PDF). SMILES data (CSV). The Supporting Information is available free of charge on the ACS Publications website at DOI: 10.1021/acs.jmedchem.5b00518.

AUTHOR INFORMATION

Corresponding Author

*Phone: +31-71-527-4651. E-mail: ijzerman@lacdr.leidenuniv.nl.

Author Contributions

Zhiyi Yu designed and conducted experiments, analyzed the data, and wrote the manuscript. Jacobus P. D. van Veldhoven, Julien Louvel, and Ingrid M. E. 't Hart synthesized the novel compounds in this study. Martin B. Rook and Marcel A. G. van der Heyden designed the patch clamp assay and assessed the results. Laura H. Heitman designed experiments, assessed the results, and wrote the manuscript. Adriaan P. IJzerman designed experiments, assessed the results, and wrote the manuscript.

Notes

The authors declare no competing financial interest.

ABBREVIATIONS USED

hERG, human ether-à-go-go-related gene; APD, action potential duration; TdP, Torsade de Pointes; C_{max}, maximum free plasma concentration; SAR, structure−affinity relationship; SKR, structure-kinetics relationship; RT, residence time; GPCR, G protein-coupled receptor; CiPA, comprehensive in vitro proarrhythmia assay; HEK293 $K_v11.1$, HEK293 cells stably transfected with the $K_v11.1$ (hERG) channel

REFERENCES

(1) Heijman, J.; Voigt, N.; Carlsson, L. G.; Dobrev, D. Cardiac safety assays. *Curr. Opin. Pharmacol.* **2014**, *15*, 16−21.

(2) Yu, Z.; IJzerman, A. P.; Heitman, L. H. $K_v11.1$ (hERG)-induced cardiotoxicity: a molecular insight from a binding kinetics study of prototypic $K_v11.1$ (hERG) inhibitors. *Br. J. Pharmacol.* **2015**, *172*, 940−945.

(3) Sanguinetti, M. C.; Tristani-Firouzi, M. hERG potassium channels and cardiac arrhythmia. *Nature* **2006**, *440*, 463−469.

(4) Vandenberg, J. I.; Perry, M. D.; Perrin, M. J.; Mann, S. A.; Ke, Y.; Hill, A. P. hERG K^+ channels: structure, function, and clinical significance. *Physiol. Rev.* **2012**, *92*, 1393−1478.

(5) Townsend, C. Is there a need to add another dimension (time) to the evaluation of the arrhythmogenic potential of new drug candidates in vitro? *Circulation* **2014**, *130*, 219−220.

(6) Hill, A. P.; Perrin, M. J.; Heide, J.; Campbell, T. J.; Mann, S. A.; Vandenberg, J. I. Kinetics of drug interaction with the $K_v11.1$ potassium channel. *Mol. Pharmacol.* **2014**, *85*, 769−776.

(7) Redfern, W.; Carlsson, L.; Davis, A.; Lynch, W.; MacKenzie, I.; Palethorpe, S.; Siegl, P.; Strang, I.; Sullivan, A.; Wallis, R. Relationships between preclinical cardiac electrophysiology, clinical QT interval prolongation and torsade de pointes for a broad range of drugs: evidence for a provisional safety margin in drug development. *Cardiovasc. Res.* **2003**, *58*, 32−45.

(8) Di Veroli, G. Y.; Davies, M. R.; Zhang, H.; Abi-Gerges, N.; Boyett, M. R. High-throughput screening of drug-binding dynamics to hERG improves early drug safety assessment. *Am. J. Physiol. Heart Circ. Physiol.* **2013**, *304*, H104−H117.

(9) Di Veroli, G. Y.; Davies, M. R.; Zhang, H.; Abi-Gerges, N.; Boyett, M. R. hERG inhibitors with similar potency but different binding kinetics do not pose the same proarrhythmic risk: implications for drug safety assessment. *J. Cardiovasc. Electrophysiol.* **2014**, *25*, 197−207.

(10) Ridley, J. M.; Milnes, J. T.; Duncan, R. S.; McPate, M. J.; James, A. F.; Witchel, H. J.; Hancox, J. C. Inhibition of the hERG K$^+$ channel by the antifungal drug ketoconazole depends on channel gating and involves the S6 residue F656. *FEBS Lett.* **2006**, *580*, 1999−2005.

(11) Schneider, E. V.; Bottcher, J.; Huber, R.; Maskos, K.; Neumann, L. Structure-kinetic relationship study of CDK8/CycC specific compounds. *Proc. Natl. Acad. Sci. U. S. A.* **2013**, *110*, 8081−8086.

(12) Markgren, P.-O.; Schaal, W.; Hämäläinen, M.; Karlén, A.; Hallberg, A.; Samuelsson, D.; Danielson, U. H. Relationships between structure and interaction kinetics for HIV-1 protease inhibitors. *J. Med. Chem.* **2002**, *45*, 5430−5439.

(13) Tummino, P. J.; Copeland, R. A. Residence time of receptor-ligand complexes and its effect on biological function. *Biochemistry* **2008**, *47*, 5481−5492.

(14) Goyal, M.; Rizzo, M.; Schumacher, F.; Wong, C. F. Beyond thermodynamics: drug binding kinetics could influence epidermal growth factor signaling. *J. Med. Chem.* **2009**, *52*, 5582−5585.

(15) Vilums, M.; Zweemer, A. J.; Yu, Z.; de Vries, H.; Hillger, J. M.; Wapenaar, H.; Bollen, I. A.; Barmare, F.; Gross, R.; Clemens, J.; Krenitsky, J.; Brussee, J.; Stamos, J.; Saunders, J.; Heitman, L. H.; IJzerman, A. P. Structure-kinetic relationships-an overlooked parameter in hit-to-lead optimization: a case of cyclopentylamines as chemokine receptor 2 antagonists. *J. Med. Chem.* **2013**, *56*, 7706−7714.

(16) Guo, D.; Xia, L.; van Veldhoven, J. P.; Hazeu, M.; Mocking, T.; Brussee, J.; IJzerman, A. P.; Heitman, L. H. Binding kinetics of ZM241385 derivatives at the human adenosine A$_{2A}$ receptor. *ChemMedChem* **2014**, *9*, 752−761.

(17) Winquist, J.; Geschwindner, S.; Xue, Y.; Gustavsson, L.; Musil, D.; Deinum, J.; Danielson, U. H. Identification of structural-kinetic and structural-thermodynamic relationships for thrombin inhibitors. *Biochemistry* **2013**, *52*, 613−626.

(18) Sager, P. T.; Gintant, G.; Turner, J. R.; Pettit, S.; Stockbridge, N. Rechanneling the cardiac proarrhythmia safety paradigm: a meeting report from the cardiac safety research consortium. *Am. Heart J.* **2014**, *167*, 292−300.

(19) Cavero, I.; Holzgrefe, H. Comprehensive in vitro proarrhythmia assay, a novel *in vitro/in silico* paradigm to detect ventricular proarrhythmic liability: a visionary 21st century initiative. *Expert Opin. Drug Saf.* **2014**, *13*, 745−758.

(20) Windisch, A.; Timin, E.; Schwarz, T.; Stork-Riedler, D.; Erker, T.; Ecker, G.; Hering, S. Trapping and dissociation of propafenone derivatives in hERG channels. *Br. J. Pharmacol.* **2011**, *162*, 1542−1552.

(21) Linder, T.; Saxena, P.; Timin, E. N.; Hering, S.; Stary-Weinzinger, A. Structural insights into trapping and dissociation of small molecules in K$^+$ channels. *J. Chem. Inf. Model.* **2014**, *54*, 3218−3228.

(22) Shagufta; Guo, D.; Klaasse, E.; de Vries, H.; Brussee, J.; Nalos, L.; Rook, M. B.; Vos, M. A.; van der Heyden, M. A.; IJzerman, A. P. Exploring chemical substructures essential for hERG K$^+$ channel blockade by synthesis and biological evaluation of dofetilide analogues. *ChemMedChem* **2009**, *4*, 1722−1732.

(23) Vilums, M.; Overman, J.; Klaasse, E.; Scheel, O.; Brussee, J.; IJzerman, A. P. Understanding of molecular substructures that contribute to hERG K$^+$ channel blockade: synthesis and biological evaluation of E-4031 analogues. *ChemMedChem* **2012**, *7*, 107−113.

(24) Louvel, J.; Carvalho, J. F.; Yu, Z.; Soethoudt, M.; Lenselink, E. B.; Klaasse, E.; Brussee, J.; IJzerman, A. P. Removal of human ether-à-go-go related gene (hERG) K$^+$ channel affinity through rigidity: a case of clofilium analogues. *J. Med. Chem.* **2013**, *56*, 9427−9440.

(25) Carvalho, J. o. F.; Louvel, J.; Doornbos, M. L.; Klaasse, E.; Yu, Z.; Brussee, J.; IJzerman, A. P. Strategies to reduce hERG K$^+$ channel blockade. Exploring heteroaromaticity and rigidity in novel pyridine analogues of dofetilide. *J. Med. Chem.* **2013**, *56*, 2828−2840.

(26) Suessbrich, H.; Waldegger, S.; Lang, F.; Busch, A. E. Blockade of hERG channels expressed in Xenopus oocytes by the histamine receptor antagonists terfenadine and astemizole. *FEBS Lett.* **1996**, *385*, 77−80.

(27) Fitzgerald, P. T.; Ackerman, M. J. Drug-induced Torsades de Pointes: the evolving role of pharmacogenetics. *Heart Rhythm* **2005**, *2*, S30−S37.

(28) Rajamani, S.; Shryock, J. C.; Belardinelli, L. Rapid kinetic interactions of ranolazine with hERG K$^+$ current. *J. Cardiovasc. Pharmacol.* **2008**, *51*, 581−589.

(29) Orita, A.; Nakano, T.; An, D. L.; Tanikawa, K.; Wakamatsu, K.; Otera, J. Metal-assisted assembly of pyridine-containing arylene ethynylene strands to enantiopure double helices. *J. Am. Chem. Soc.* **2004**, *126*, 10389−10396.

(30) Nishihara, Y.; Noyori, S.; Okamoto, T.; Suetsugu, M.; Iwasaki, M. Copper-catalyzed Sila-Sonogashira-Hagihara cross-coupling reactions of alkynylsilanes with aryl iodides under palladium-free conditions. *Chem. Lett.* **2011**, *40*, 972−974.

(31) Siemsen, P.; Livingston, R. C.; Diederich, F. Acetylenic Coupling: A Powerful Tool in Molecular Construction. *Angew. Chem., Int. Ed.* **2000**, *39*, 2632−2657.

(32) Shen, X.; Ho, D. M.; Pascal, R. A. Synthesis of polyphenylene dendrimers related to "cubic graphite. *J. Am. Chem. Soc.* **2004**, *126*, 5798−5805.

(33) Aggarwal, A. V.; Jester, S. S.; Taheri, S. M.; Förster, S.; Höger, S. Molecular Spoked Wheels: Synthesis and Self-Assembly Studies on Rigid Nanoscale 2D Objects. *Chem. - Eur. J.* **2013**, *19*, 4480−4495.

(34) Motulsky, H. J.; Mahan, L. The kinetics of competitive radioligand binding predicted by the law of mass action. *Mol. Pharmacol.* **1984**, *25*, 1−9.

(35) Cheng, Y.-C.; Prusoff, W. H. Relationship between the inhibition constant (K_I) and the concentration of inhibitor which causes 50% inhibition (I_{50}) of an enzymatic reaction. *Biochem. Pharmacol.* **1973**, *22*, 3099−3108.

(36) Jamieson, C.; Moir, E. M.; Rankovic, Z.; Wishart, G. Medicinal chemistry of hERG optimizations: highlights and hang-ups. *J. Med. Chem.* **2006**, *49*, 5029−5046.

(37) Fernandez, D.; Ghanta, A.; Kauffman, G. W.; Sanguinetti, M. C. Physicochemical features of the hERG channel drug binding site. *J. Biol. Chem.* **2004**, *279*, 10120−10127.

(38) Zhu, B.; Jia, Z. J.; Zhang, P.; Su, T.; Huang, W.; Goldman, E.; Tumas, D.; Kadambi, V.; Eddy, P.; Sinha, U.; Scarborough, R. M.; Song, Y. Inhibitory effect of carboxylic acid group on hERG binding. *Bioorg. Med. Chem. Lett.* **2006**, *16*, 5507−5512.

(39) Cavalli, A.; Buonfiglio, R.; Ianni, C.; Masetti, M.; Ceccarini, L.; Caves, R.; Chang, M. W.; Mitcheson, J. S.; Roberti, M.; Recanatini, M. Computational design and discovery of "minimally structured" hERG blockers. *J. Med. Chem.* **2012**, *55*, 4010−4014.

(40) Mitcheson, J. S.; Chen, J.; Lin, M.; Culberson, C.; Sanguinetti, M. C. A structural basis for drug-induced long QT syndrome. *Proc. Natl. Acad. Sci. U. S. A.* **2000**, *97*, 12329−12333.

(41) Czodrowski, P. hERG me out. *J. Chem. Inf. Model.* **2013**, *53*, 2240−2251.

(42) Pearlstein, R. A.; Vaz, R. J.; Kang, J.; Chen, X.; Preobrazhenskaya, M.; Shchekotikhin, A. E.; Korolev, A. M.; Lysenkova, L. N.; Miroshnikova, O. V.; Hendrix, J.; Rampe, D. Characterization of hERG potassium channel inhibition using CoMSiA 3D QSAR and homology modeling approaches. *Bioorg. Med. Chem. Lett.* **2003**, *13*, 1829−1835.

(43) Kramer, C.; Beck, B.; Kriegl, J. M.; Clark, T. A composite model for hERG blockade. *ChemMedChem* **2008**, *3*, 254−265.

(44) Farid, R.; Day, T.; Friesner, R. A.; Pearlstein, R. A. New insights about hERG blockade obtained from protein modeling, potential energy mapping, and docking studies. *Bioorg. Med. Chem.* **2006**, *14*, 3160−3173.

(45) Aronov, A. M. Predictive in silico modeling for hERG channel blockers. *Drug Discovery Today* **2005**, *10*, 149−155.

(46) Jiang, Y.; Lee, A.; Chen, J.; Ruta, V.; Cadene, M.; Chait, B. T.; MacKinnon, R. X-ray structure of a voltage-dependent K^+ channel. *Nature* **2003**, *423*, 33−41.

(47) Abraham, J. C. M. M.; Vekstein, C.; Lawrence, D.; Bhargava, M.; Janiszewski, D.; Militello, M.; Nissen, S.; Poe, S.; Saliba, W.; Tanaka-Esposito, C.; Wolski, K.; Wilkoff, B. Safety of oral dofetilide loading for rhythm control of atrial arrhythmias. *J. Am. Coll. Cardiol.* **2014**, *63*, A435.

(48) Ficker, E.; Jarolimek, W.; Kiehn, J.; Baumann, A.; Brown, A. M. Molecular determinants of dofetilide block of hERG K^+ channels. *Circ. Res.* **1998**, *82*, 386−395.

(49) Guo, D.; Mulder-Krieger, T.; IJzerman, A. P.; Heitman, L. H. Functional efficacy of adenosine A_{2A} receptor agonists is positively correlated to their receptor residence time. *Br. J. Pharmacol.* **2012**, *166*, 1846−1859.

(50) Yu, Z.; Klaasse, E.; Heitman, L. H.; IJzerman, A. P. Allosteric modulators of the hERG K^+ channel: Radioligand binding assays reveal allosteric characteristics of dofetilide analogs. *Toxicol. Appl. Pharmacol.* **2014**, *274*, 78−86.